

Gyrokinetic Theory of Linear Gravitational Flute Interchanges with Flow Shear Stabilization

Z. Y. Tan^{1,2†}, and I. G. Abel^{2,3}

¹Department of Physics, University of Maryland, College Park, Maryland 20742, USA

²Institute for Research in Electronics & Applied Physics, University of Maryland, College Park, MD 20740, USA

³Gridfire Inc, 3422 Old Capitol Trail, Suite 700, Wilmington, DE 19808, USA

(Received xx; revised xx; accepted xx)

A collisionless electrostatic gyrokinetic theory is developed to describe how the presence of a differential velocity shear can help stabilize linear gravitational flute interchanges in slab geometry. This is made possible because the velocity shear acts to increase the perpendicular wavenumber of the unstable modes with time. Eventually, a threshold wavenumber is crossed where the effect of gyroaveraging, captured by the J_0 Bessel function in the gyrokinetic equation, results in a damping of the instability by nature of J_0 being a decaying sinusoidal. However, transient amplification, responsible for subcritical turbulence, can still occur. Numerical comparisons are made with a Magnetohydrodynamic model with gyroviscous corrections as well as the GX gyrokinetic code. It is demonstrated that an increasing shear acts not only to accelerate the stabilization effect but also to reduce the overall transient amplification.

1. Introduction

The gravitational interchange instability was first analyzed by Kruskal & Schwarzschild (1954) using ideal Magnetohydrodynamics (MHD). This instability arises in configurations where when the mean density gradient ∇n of the plasma is in the opposite direction to the gravitational field $\mathbf{g} = -g\hat{x}$ as depicted in Figure 1. In this setup, we consider a quasineutral plasma in slab geometry, with a constant magnetic field $\mathbf{B} = B\hat{b} = B\hat{z}$ threading it such that $\mathbf{g} \perp \mathbf{B}$. Since part of the Larmor orbit is against the gravitational field, this gives rise to a ‘gravitational drift’ $\mathbf{g} \times \hat{b}/\Omega_s = g\hat{y}/\Omega_s$ where Ω_s is the gyrofrequency of a particle of species s (Goldston & Rutherford 1995). Because $m_e \ll m_i$, this drift affects the ions more than the electrons and this leads to charge separation when there is a wave-like perturbation in the presence of a density gradient. As depicted in Figure 1, the resulting perturbed electric field $\delta\mathbf{E}$ and its corresponding drift amplifies the perturbation, causing an instability. This instability is purely electrostatic and does not perturb the magnetic field.

The first attempt to include finite Larmor radius (FLR) effects into the theory of this instability was performed by Rosenbluth *et al.* (1962) using Vlasov theory. Their result predicted a $\mathcal{O}(k_\perp \rho_i)$ correction to the original dispersion relation of Kruskal & Schwarzschild (1954) where k_\perp is the perpendicular wavenumber and ρ_i is the thermal ion Larmor radius. While the ideal MHD result predicted no stable modes, the correction resulted in a threshold value of $k_\perp \rho_i$, beyond which the modes are stable. This is known as ‘FLR stabilization’ and it was reproduced by Roberts & Taylor (1962) by modifying the stress

† Email address for correspondence: zytan@umd.edu

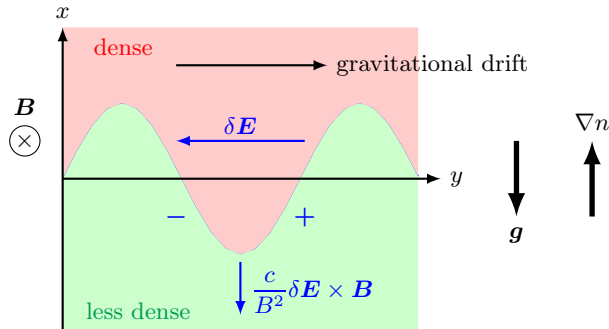


FIGURE 1: Schematic of plasma setup in slab geometry for the onset of the gravitational flute interchange instability. \mathbf{B} is the mean magnetic field (into the page), $\mathbf{g} = -g\hat{x}$ is the gravitational field, and ∇n is the density gradient. A wavelike perturbation (in blue) in the xy plane breaks the translational symmetry in y , leading to a charge build up (indicated by the ‘-’ and ‘+’ symbols) due to the gravitational drift in which an opposing perturbed electric field $\delta\mathbf{E}$ must be set up to maintain quasineutrality; however, the resulting $c\delta\mathbf{E} \times \mathbf{B}/B^2$ drift amplifies the perturbation leading to an instability. The density gradient is necessary to ensure that $\delta\mathbf{E}$ is pointing in the right direction. If the density gradient was opposite to that in the diagram, then direction of $\delta\mathbf{E}$ would be flipped, resulting in a restoring rather than destabilizing drift.

tensor in the the ideal MHD momentum equation. This modification is known as the gyroviscous stress and it was first identified by Thompson (1961) and more rigorously treated by Braginskii (1965) in the context of collisional plasmas. Since then, a great deal of research has gone into modeling and understanding FLR stabilization for the gravitationally driven interchange (Rosenbluth & Simon 1965; Bowers & Haines 1968; Ariel & Bhatia 1969; Huba 1996; Schnack *et al.* 2006; Ferraro 2006, 2007; Xu & Kunz 2016).

In the context of fusion devices, gravitational effects are generally negligible; however, from our description in the beginning, we see that the instability may be induced from any drift that affects ions and electrons differently, such as the curvature or ∇B drifts. The presence of such interchanges in these devices makes them interesting to study (Rosenbluth & Longmire 1957; Wakatani *et al.* 1992; Zagórski *et al.* 1999; Tatsuno *et al.* 1999; Levitt 2004; Poli *et al.* 2008). Of particular interest is the centrifugal mirror, where plasma rotation is imposed in order to confine the plasma (Lehnert 1971; Hassam 1997; Ellis *et al.* 2001; Teodorescu *et al.* 2008). The idea is that in the co-rotating frame, particles experiences a centrifugal force. The component of this force perpendicular to mirror field lines is balanced by the $\mathbf{J} \times \mathbf{B}$ force that manifests from the plasma rotation. On the other hand, the parallel component is unbalanced and its direction is pointing towards the center of the device, thereby confining the plasma.

Unfortunately, because the electron centrifugal drift is negligible due to its small mass, it is mainly the ions that are affected (Goldston & Rutherford 1995; Levitt 2004; Abel *et al.* 2013). Consequentially, this centrifugal drift can drive the interchange instability. However, the rotational shear can induce FLR stabilization (Hassam 1992; Ellis *et al.* 2001; Huang & Hassam 2001) by tilting the unstable modes and pushing $k_{\perp}\rho_i$ past the aforementioned threshold as seen in Figure 2. What results is that the stability depends on the competition between the destabilizing centrifugal drive and the stabilizing shear.

The idea of utilizing sheared flows to suppress instabilities and turbulence has been researched thoroughly throughout the years (Biglari *et al.* 1990; Artun & Tang 1992; Waltz *et al.* 1998; Hobbs *et al.* 2001; Newton *et al.* 2010; Ivanov *et al.* 2025).

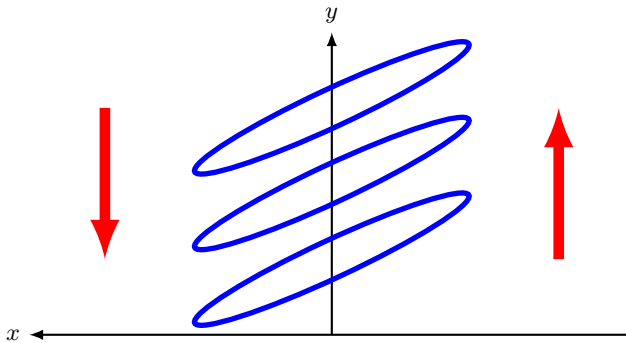


FIGURE 2: The presence of differential flow shear \mathbf{u} (red arrows) causes the linear modes (in blue) to ‘tilt’ overtime, resulting in $k_{\perp}\rho_i$ increasing until possibly crossing the threshold value for FLR stabilization.

However, even if the shear stabilization ensures that all modes are eventually stable, it is still possible for a stable mode to experience an initial positive growth before decaying. This is known as linear transient amplification and it is a possible driver of a phenomenon known as ‘subcritical turbulence’ i.e. turbulence in the absence of linear instabilities (Highcock *et al.* 2010, 2011; Barnes *et al.* 2011; Schekochihin *et al.* 2012; Landreman *et al.* 2015). Study of this feature is very relevant for the problem at hand, since some time is needed before the shear pushes the modes into the FLR stabilization regime, during which, transient amplification can occur. This was demonstrated by Ng & Hassam (2005) and will become apparent in the numerical solutions in this work.

However, because the model by Ng & Hassam (2005) only provides $\mathcal{O}(k_y\rho_i)$ corrections to the MHD model by Kruskal & Schwarzschild (1954) (which takes $k_y\rho_i \rightarrow 0$), it is natural to question its validity as $k_{\perp}\rho_i \rightarrow 1$ due to the shear. This is the theoretical motivation for this paper, which is to model the interchange using gyrokinetics (Antonsen & Lane 1980; Friemen & Chen 1982; Catto *et al.* 1981; Abel *et al.* 2013), which naturally provides $k_y\rho_i$ corrections to all orders. This linear flow shear problem, in the framework of gyrokinetics, can then be analyzed using the theory developed by Schekochihin *et al.* (2012) for ion temperature gradient and parallel velocity gradient instabilities.

We shall organize the paper as follows. In §2, we will describe the setup and assumptions made in the paper. In §3, we will demonstrate how the $\mathcal{O}(k_y\rho_i)$ correction in gyroviscous MHD leads to FLR stabilization for the interchange in the absence of shear. Also, we will derive a time-dependent model to describe the problem with flow shear. These are then repeated in §4, but this time using gyrokinetics. We will then compare the solutions from MHD and gyrokinetics with the GX gyrokinetic code Mandell *et al.* (2018, 2024) in §5. Finally, we will conclude with a summary and a discussion on future work in §6. We note that, throughout this paper, our notation will adhere strictly to Abel *et al.* (2013) and Schekochihin *et al.* (2012) as far as possible. Any deviations will be highlighted in the paper.

2. Assumptions and Setup

We draw the following assumptions from the previous studies on the interchange instability mentioned in the introduction. Firstly, we will consider a quasineutral hydrogen plasma $Z_i = +1, Z_e = -1, n_e = n_i$ where Z_i is the ionic charge, Z_e is the electron charge,

and n_s is the mean density of species s . We assume that the variation of n_s is purely in the \hat{x} direction i.e. $n_s = n_s(x)$ and that no temperature gradient exists so that the focus is solely on the interaction between the density gradient and the gravitational field. The plasma will be also assumed to be thermally equilibrated i.e. $T_i = T_e$ where T_i and T_e are the ion and electron temperatures respectively.

Secondly, as depicted in Figure 1, the plasma is subjected to a uniform mean magnetic field $\mathbf{B} = B\hat{\mathbf{b}} = B\hat{\mathbf{z}}$ and a constant gravitational field $\mathbf{g} = -g\hat{\mathbf{x}}$ in which $g \sim v_{\text{th},i}^2/a_N$ (Ng & Hassam 2005). Here, $v_{\text{th},s} = \sqrt{2T_s/m_s}$ is the thermal velocity of a particle of species s and a_N is the characteristic length scale of the plasma. In addition, we will consider a linear shear $\mathbf{u} = Sx\hat{\mathbf{y}}$ with S being the shear parameter (Schekochihin *et al.* 2012).

Thirdly, as explained in the introduction, we consider purely electrostatic fluctuations i.e. $\delta\mathbf{B} = 0$. Moreover, we will only consider the most unstable interchanges (flutes), which are fundamentally 2D perturbations with $k_{\parallel} \rightarrow 0$ (Rosenbluth & Simon 1965; Hassam 1992), with k_{\parallel} being the parallel wavenumber. Consequentially, we need to consider full kinetic electrons since the parallel streaming needed for an adiabatic response is now not possible.

Fourthly, we shall focus solely on the linear collisionless theory as was done in earlier references (Rosenbluth *et al.* 1962; Roberts & Taylor 1962; Ng & Hassam 2005). It is worth noting that the ‘collision-free’ approximation of the Braginskii stress tensor is simply the aforementioned gyroviscosity (Roberts & Taylor 1962; Schnack *et al.* 2006; Parra 2019). Also, even though MHD fundamentally requires collisions, the collisionless assumption in our theory is still valid for two reasons: First, the primary difference between a collisional and collisionless model is the presence of Landau damping (Xu & Kunz 2016), which our problem does not contain because we have taken $k_{\parallel} \rightarrow 0$.¹ Second, the perpendicular dynamics of the plasma is still fluid-like even in the absence of collisions, provided that $\omega \ll \Omega_i$ and $k_{\perp}\rho_i \ll 1$ (Thompson 1961; Schekochihin *et al.* 2009).

Lastly, we shall work with the low Mach number limit of gyrokinetics (Abel *et al.* 2013) such that we can independently control the shear and the gravitational drive.² As we shall soon see, if we do not consider this limit, the ‘shearing box transformation’ performed in §3.2.1 will not be able to cleanly remove the shear S from our equations due to the presence of centrifugal effects in the gyrokinetic equation, resulting in additional complexities.

3. The MHD interchange with gyroviscosity

The goal of this section is to understand how, in the absence of flow shear, FLR stabilization arises when gyroviscosity is included in ideal MHD and how it introduces a threshold perpendicular wavenumber, beyond which the modes become stable. In addition, a finite-flow-shear time-dependent MHD model will also be derived. This model will be later used in §5 to demonstrate how a mode with an initially unstable perpendicular wavenumber can be made stable with flow shear. This happens because the flow shear will eventually push the wavenumber past the aforementioned threshold.

The finite-flow-shear model in this section is similar to that of Ng & Hassam (2005);

¹Note that we have taken the ion mean free path λ_{mfpi} to be large enough such that $k_{\parallel}\lambda_{\text{mfpi}} \gg 1$ in order to maintain the collisionless property of the plasma.

²The low Mach number model in Abel *et al.* (2013) is the intermediate limit where $\epsilon \ll M \ll 1$. However, we shall later see in (A9) that for this problem, the regime of interest is the ‘low flow regime’ where $M \sim \epsilon$. Nevertheless, it will become apparent in §4.3 that this is of no issue as the goal is to remove explicit presence of the shear S in the gyrokinetic equation via the ‘shearing box transformation’ described in §3.2.1, which occurs regardless of which regime of M you consider.

however, we have elected to re-derive the time-dependent equations from the MHD equations used in Roberts & Taylor (1962) which, unlike Ng & Hassam (2005), does not assume incompressibility of the plasma. The reason is that it will be later demonstrated that, at zero shear, it is the latter that produces the same dispersion relation as in gyrokinetics. As gyrokinetics is the focus of our paper, we shall leave the full derivation of our MHD model to Appendix A and only quote results from it.

3.1. FLR stabilization in the absence of flow shear

The original calculation of the interchange modes by Kruskal & Schwarzschild (1954), using the linearized ideal MHD equations and assuming the perturbed quantities to be of the form $e^{ik_y y + i\omega t}$, demonstrated that the modes were unstable. These modes were found to have a growth rate equal to

$$\gamma_g = \sqrt{\frac{\omega_{*i}\omega_{gi}}{k_y^2 \rho_i^2 / 2}} = \sqrt{g \frac{d \ln n_i}{dx}}, \quad (3.1)$$

where we have defined the frequencies

$$\omega_{*s} = \frac{v_{\text{th},s}}{2} k_y \rho_s \frac{d \ln n_s}{dx}, \quad (3.2)$$

and

$$\omega_{gs} = \frac{g}{v_{\text{th},s}} k_y \rho_s, \quad (3.3)$$

where s is the species index. Later calculations by Rosenbluth *et al.* (1962) using Vlasov theory derived a $\mathcal{O}(k_y \rho_i)$ correction to the ideal MHD dispersion relation:

$$\omega^2 = -\frac{\omega_{gi}\omega_{*i}}{k_y^2 \rho_i^2 / 2} + \underbrace{(\omega_{gi} + \omega_{*i})\omega}_{\mathcal{O}(k_y \rho_i)} + \mathcal{O}(k_y^2 \rho_i^2), \quad (3.4)$$

this result was later repeated by Roberts & Taylor (1962), using MHD but modifying the momentum equation to include gyroviscous stress (Braginskii 1965; Parra 2019).

The derivation of (3.4) can be found in §A.3. In this derivation, we have repeated the calculation in Roberts & Taylor (1962), but allowed for $k_x \neq 0$. What follows is that the denominator of the first term on the RHS of (3.4) is replaced by $k_\perp^2 \rho_i^2 / 2$. This implies that having $k_x \neq 0$ contributes to the stability of the mode. Our focus will be on the most unstable modes in which $k_x = 0$ and hence $k_\perp = k_y$.

We also note here that the $\mathcal{O}(k_y \rho_i)$ correction in (3.4) differs from equation (13) in Ng & Hassam (2005) in which the latter does not possess the $\omega_{gi}\omega$ term. As demonstrated in Appendix B, this difference arises from the incompressibility assumption made in Ng & Hassam (2005).

The dispersion relation (3.4) can be solved to give

$$\omega = \frac{1}{2} \left[(\omega_{gi} + \omega_{*i}) \pm \sqrt{(\omega_{gi} + \omega_{*i})^2 - 4 \frac{\omega_{gi}\omega_{*i}}{k_y^2 \rho_i^2 / 2}} \right], \quad (3.5)$$

we see that the system is stable when

$$(\omega_{gi} + \omega_{*i})^2 \geq \frac{8\omega_{gi}\omega_{*i}}{k_y^2 \rho_i^2} \implies |k_y \rho_i| \geq \frac{\sqrt{8\omega_{gi}\omega_{*i}}}{\omega_{gi} + \omega_{*i}}. \quad (3.6)$$

Equation (3.6) defines the threshold value of $k_y \rho_i$ (equivalently $k_\perp \rho_i$) for FLR stabilization that we have previously mentioned. This was absent in (3.1) and arises due to the

addition of gyroviscosity to the MHD momentum equation which accounts for first order FLR corrections (see §A.3).

In the next section, we outline a time-dependent theory in MHD with finite flow shear which predicts that an initially unstable mode with $k_x = 0$ will evolve to have a finite k_x and eventually become stable when $k_\perp \rho_i$ satisfies (3.6).

3.2. Finite flow shear

3.2.1. Shearing boxes and time-dependent wavenumbers

Let us first demonstrate how flow shear causes the wavenumbers $k_\perp \rho_i$ to increase. We introduce the ‘shearing box transformation’ (Schekochihin *et al.* 2012; Fox *et al.* 2017) which corresponds to a coordinate transformation $(t, \mathbf{r}) \rightarrow (t', \mathbf{r}')$ to a local orthogonal Cartesian frame, moving with and in the vicinity of some flux surface.¹ As mentioned in §2, we are considering a linear shear $\mathbf{u} = Sx\hat{\mathbf{y}}$ and the transformation is given by:

$$t' = t, \quad x' = x, \quad y' = y - Sxt, \quad z' = z. \quad (3.7)$$

As seen in §A.4, this transformation removes the spatial and S dependence from the coefficients of the linearized MHD equations. This allows us to utilize the normal mode solutions as was done in the zero shear scenario. However, as the problem is now time-dependent, we do not assume $e^{i\omega t}$ time-dependence, since the growth rates will also be time-dependent. Instead, any perturbative quantity assumes the form:

$$X(\mathbf{r}', t') = \hat{X}(t') e^{i\mathbf{k}'_\perp \cdot \mathbf{r}'} = \hat{X}(t') e^{i\mathbf{k}_\perp \cdot (\mathbf{k}'_\perp, t') \cdot \mathbf{r}}, \quad (3.8)$$

where we remind the reader that we have taken $k_\parallel = k_z \rightarrow 0$ for flute modes.

From the respective partial derivatives, we see that $k_y = k'_y$ and more importantly:

$$k_x = k_x(t) = k'_x - St'k'_y. \quad (3.9)$$

This demonstrates the time-dependent property of k_x due to flow shear. As we explained in the zero shear case, we can set $k'_x = 0$ to focus on the most unstable modes. However, even though we will initially have $k_x = k'_x = 0$, $|k_x|$ will increase over time as $S \neq 0$ according to (3.9), meaning that k_x will not remain zero.

This immediately poses a challenge for the gyroviscous MHD model which assumes $k_\perp \rho_i \ll 1$ and only provides a $\mathcal{O}(k_\perp \rho_i)$ correction. As t gets large, it is clear from (3.9) that we will eventually reach $k_\perp \rho_i \sim 1$ at which point our MHD theory breaks down. This is the motivation for a gyrokinetic treatment which does not suffer the same predicament.

3.2.2. Time-dependent equation

The original derivation of the finite-flow-shear time-dependent MHD equation was calculated by Ng & Hassam (2005). However, as mentioned in §3.1, because of the incompressibility assumption made in their paper, the $\mathcal{O}(k_y \rho_i)$ correction to the zero shear dispersion relation differs from that of Rosenbluth *et al.* (1962) and Roberts & Taylor (1962) which is given by (3.4). More importantly, we will later see in §4.2, that it is (3.4) which agrees with our derivation of the analogous zero shear dispersion relation in gyrokinetics up to $\mathcal{O}(k_y \rho_i)$.

For the above reasons, we have chosen to re-derive the time-dependent equation using the extended MHD equations in Roberts & Taylor (1962) that replaces the incompressibility condition with the generalized Ohm’s law. Substituting the solutions (3.8) into these equations, solving for the perturbed ion density $\widehat{\delta n}_i$, and suppressing all the primes

¹In our case, the ‘flux surfaces’ are planes labeled by x .

gives us

$$\begin{aligned} \frac{\partial^2 \widehat{\delta n}_i(t)}{\partial t^2 \widehat{\delta n}_i(0)} + \left[\frac{2S^2 t}{S^2 t^2 + 1} - i(\omega_{gi} + \omega_{*i}) \right] \frac{\partial \widehat{\delta n}_i(t)}{\partial t \widehat{\delta n}_i(0)} \\ - \frac{1}{S^2 t^2 + 1} \left[i(2\omega_{gi} + \omega_{*i}) S^2 t + \frac{\omega_{gi} \omega_{*i}}{k_y^2 \rho_i^2 / 2} \right] \frac{\widehat{\delta n}_i(t)}{\widehat{\delta n}_i(0)} = 0. \end{aligned} \quad (3.10)$$

The derivation of this equation can be found in §A.4. Though we have derived an $\mathcal{O}(k_y^2 \rho_i^2)$ equation in (A 33), we have elected to use only the $\mathcal{O}(k_y \rho_i)$ equations for reasons that will be explained in §4.2.

3.2.3. Short-time limit

In the short-time limit, because we expect the effects of shear to be weak, the time-dependent equation (3.10) should therefore reduce to equation (3.1). This regime is characterized by considering the limit $St \ll 1$ in equation (3.4). The reason why this is chosen as opposed to $t \ll 1$ is explained in more detail in §3.1 of Schekochihin *et al.* (2012). Upon taking this limit and assuming solutions of the form $e^{ik_y y + i\omega t}$, it can be shown that (3.1) is indeed recovered. Outside the short-time regime, we need to solve equation (3.10) numerically. However, this will be deferred to §5 as we want to first introduce our gyrokinetic model which is the main objective of this paper.

4. Gyrokinetic theory of gravitational flute interchanges

In the previous section, we used MHD with gyroviscosity to obtain a $\mathcal{O}(k_y \rho_i)$ correction to the ideal MHD dispersion relation. We saw that in the case of finite flow shear $S \neq 0$, $k_\perp \rho_i$ becomes time-dependent and eventually increases past a point where $k_\perp \rho_i \sim 1$ in which the $\mathcal{O}(k_y \rho_i)$ correction no longer suffices. To account for this shortfall, we shall now use gyrokinetics, which retains all orders of $k_y \rho_i$.

4.1. Linear collisionless gyrokinetic equation with gravity

The inclusion of gravity results in an additional drift term $\mathbf{g} \cdot \partial f_s / \partial \mathbf{v}$ on the LHS of the usual Fokker-Planck kinetic equation. Following the systematic procedure in Abel *et al.* (2013), we may then convert the equation to rotating gyrokinetic variables: the guiding-centre position \mathbf{R}_s , particle energy ε_s , magnetic moment μ_s , and the gyrophase ϑ . Next, we perform a perturbative expansion of the Fokker-Planck equation to $\mathcal{O}(\epsilon^2 \Omega_s f_s)$ where $\epsilon = \rho_i / a_N$ is the gyrokinetic expansion parameter with a_N being the characteristic length scale of the system. Finally, considering only the fluctuating part of the equation, ignoring collisions, and neglecting products of fluctuating quantities, we obtain the following linear collisionless gyrokinetic equation in the *low Mach number* limit¹:

$$\begin{aligned} \left[\frac{\partial}{\partial t} + \mathbf{u}(\mathbf{R}_s) \cdot \frac{\partial}{\partial \mathbf{R}_s} \right] h_s + \left(w_\parallel \hat{\mathbf{z}} + \frac{g}{\Omega_s} \hat{\mathbf{y}} \right) \cdot \frac{\partial h_s}{\partial \mathbf{R}_s} \\ = \frac{Z_s e F_{0s}}{T_s} \left[\frac{\partial}{\partial t} + \mathbf{u}(\mathbf{R}_s) \cdot \frac{\partial}{\partial \mathbf{R}_s} \right] \langle \delta \varphi \rangle_{\mathbf{R}} + \frac{c F_{0s}}{B} \left(\frac{d \ln n_s}{dx} + \frac{m_s g}{T_s} \right) \hat{\mathbf{y}} \cdot \frac{\partial \langle \delta \varphi \rangle_{\mathbf{R}}}{\partial \mathbf{R}_s}. \end{aligned} \quad (4.1)$$

This equation is analogous to equation (248) in Abel *et al.* (2013), modified to include gravitational effects. Here, $\langle \cdot \rangle_{\mathbf{R}}$ indicates a gyroaveraged quantity, $\delta \varphi$ is the fluctuating

¹The flux surface label and the symmetry direction are defined to be $\psi = Bax$ and $\nabla \phi = \hat{\mathbf{y}}/a$ respectively in order to draw parallels with the toroidal decomposition of the magnetic field ($\mathbf{B} = \nabla \psi \times \nabla \phi$) found in Abel *et al.* (2013).

electrostatic potential, and w_{\parallel} is the parallel *peculiar velocity* of the particle², and F_{0s} is the equilibrium Maxwellian distribution given by:

$$F_{0s}(x(\mathbf{R}_s), \varepsilon_s) = \frac{n_s(x(\mathbf{R}_s))}{\pi^{3/2} v_{\text{th},s}^3} e^{m_s g x / T_s} e^{-m_s w^2 / 2 T_s}. \quad (4.2)$$

The quantity h_s represents the gyrophase-independent distribution of Larmor rings of species s which is related to the overall distribution function f_s by:

$$f_s = F_{0s} + \delta f_s = F_{0s} - \frac{Z_s e \delta \varphi}{T_s} F_{0s} + h_s. \quad (4.3)$$

It is worthwhile to note that unlike in Abel *et al.* (2013), we do not possess the $\mathcal{O}(\epsilon)$ correction to the mean electric field \mathbf{E} , which they denote as φ_0 . This correction arises due to centrifugal and Coriolis effects, both of which are absent in our problem due to the simplified slab geometry.

The gyrokinetic equation (4.1) contains two unknowns h_s and $\langle \delta \varphi \rangle_{\mathbf{R}}$. We close the system with the quasineutrality condition:

$$\sum_s \frac{Z_s^2 e^2 n_s}{T_s} \delta \varphi = \sum_s Z_s e \int d^3 \mathbf{w} \langle h_s \rangle_{\mathbf{r}}. \quad (4.4)$$

Motivated by our earlier analysis in MHD, we shall first consider the case of zero shear and then move on to consider finite shear.

4.2. Zero flow shear

First, we consider the scenario where $\mathbf{u} = 0$. In this case, (4.1) becomes

$$\frac{\partial h_s}{\partial t} + \left(w_{\parallel} \hat{\mathbf{z}} + \frac{g}{\Omega_s} \hat{\mathbf{y}} \right) \cdot \frac{\partial h_s}{\partial \mathbf{R}_s} = \frac{Z_s e F_{0s}}{T_s} \frac{\partial \langle \delta \varphi \rangle_{\mathbf{R}}}{\partial t} + \frac{c F_{0s}}{B} \left(\frac{d \ln n_s}{dx} + \frac{m_s g}{T_s} \right) \hat{\mathbf{y}} \cdot \frac{\partial \langle \delta \varphi \rangle_{\mathbf{R}}}{\partial \mathbf{R}_s}. \quad (4.5)$$

As done in MHD, we seek solutions of the form (A 18), setting $k_x = 0$ for the most unstable modes as previously discussed:

$$\delta \varphi(\mathbf{r}, t) = \widehat{\delta \varphi} e^{i k_y y - i \omega t}, \quad (4.6)$$

$$h_s(\mathbf{R}_s, t) = \hat{h}_s e^{i k_y \mathbf{R}_s \cdot \hat{\mathbf{y}} - i \omega t}. \quad (4.7)$$

Our flux surface label in this problem can be defined as $\psi = \psi(x) = B a x$. Because we intend to later perform the ‘shearing box transformation’ discussed in §3.2.1 for the case of finite shear (which is an expansion in the vicinity of some flux surface), we perform a local approximation about $x = 0$ (Rosenbluth *et al.* 1962) by considering $x \sim \rho_i$. As a result, we can drop the $m_s g x \sim \epsilon T_s$ term in the exponent of the Maxwellian in (4.2) and simply have $F_{0s} = n_s e^{-w^2 / v_{\text{th},s}^2} / (\pi v_{\text{th},s}^2)^{3/2}$.

The gyroaverages of $\delta \varphi$ and h_s are then computed in the usual way:

$$\langle \delta \varphi \rangle_{\mathbf{R}} = \widehat{\delta \varphi} e^{i k_y \mathbf{R}_s \cdot \hat{\mathbf{y}} - i \omega t} J_0 \left(\frac{w_{\perp} k_y}{\Omega_s} \right), \quad (4.8)$$

$$\langle h_s \rangle_{\mathbf{r}} = \hat{h}_s e^{i k_y y - i \omega t} J_0 \left(\frac{w_{\perp} k_y}{\Omega_s} \right), \quad (4.9)$$

where we note that h_s is gyroaveraged at fixed \mathbf{r} while $\delta \varphi$ is gyroaveraged at fixed \mathbf{R}_s . Substituting (4.7) and (4.8) into the gyrokinetic equation (4.5) gives us an equation for

²The peculiar velocity \mathbf{w} is related to the actual particle velocity \mathbf{v} via $\mathbf{w} = \mathbf{v} - \mathbf{u}$.

\hat{h}_s :

$$\hat{h}_s = \frac{Z_s e}{T_s} \left(\frac{\omega - \omega_{*s} - \omega_{gs}}{\omega - \omega_{gs}} \right) J_0 \left(\frac{w_\perp k_y}{\Omega_s} \right) F_{0s} \widehat{\delta\varphi}, \quad (4.10)$$

where ω_{gs} and ω_{*i} were previously defined in (3.2) and (3.3) respectively.

Substituting (4.6), (4.9), and (4.10) into the quasineutrality condition (4.4) gives us

$$\sum_s \frac{Z_s^2 e^2 n_s}{T_s} = \sum_s \frac{Z_s^2 e^2}{T_s} \frac{n_s}{\pi^{3/2} v_{\text{th},s}^3} \left(\frac{\omega - \omega_{*s} - \omega_{gs}}{\omega - \omega_{gs}} \right) \int d^3 \mathbf{w} \left[J_0 \left(\frac{w_\perp k_y}{\Omega_s} \right) \right]^2 e^{-w^2/v_{\text{th},s}^2}. \quad (4.11)$$

The w_\parallel integral is simply a Gaussian integral while the w_\perp integral can be evaluated by utilizing the following identity (Abramowitz & Stegun 1970):

$$\int_0^\infty dx \left[x J_n(px) J_n(qx) e^{-a^2 x^2} \right] = \frac{1}{2a^2} I_n \left(\frac{pq}{2a^2} \right) \exp \left(-\frac{p^2 + q^2}{4a^2} \right), \quad (4.12)$$

where J_n and I_n are the Bessel functions and modified Bessel functions of the first kind, respectively. This allows us to obtain the following dispersion relation

$$\sum_s \frac{Z_s^2 e^2 n_s}{T_s} = \sum_s \frac{Z_s^2 e^2 n_s}{T_s} \frac{\omega - \omega_{gs} - \omega_{*s}}{\omega - \omega_{gs}} I_0 \left(\frac{k_y^2 \rho_s^2}{2} \right) e^{-k_y^2 \rho_s^2 / 2}. \quad (4.13)$$

4.2.1. Long wavelength and small mass ratio limit

We will now demonstrate how the zero shear dispersion relation in MHD from §3.1 can be recovered from (4.13). For a hydrogen plasma, taking the long wavelength limit i.e. $k_y \rho_i \ll 1$ and hence $I_0(k_y^2 \rho_i^2 / 2) e^{-k_y^2 \rho_i^2 / 2} \approx 1 - k_y^2 \rho_i^2 / 2$ results in (4.13) becoming:

$$\frac{1}{T_i} + \frac{1}{T_e} = \frac{1}{T_i} \frac{\omega - \omega_{gi} - \omega_{*i}}{\omega - \omega_{gi}} \left(1 - \frac{k_y^2 \rho_i^2}{2} \right) + \frac{1}{T_e} \frac{\omega - \omega_{ge} - \omega_{*e}}{\omega - \omega_{ge}} \left(1 - \frac{k_y^2 \rho_e^2}{2} \right). \quad (4.14)$$

Taking $m_e/m_i \ll 1$ and noting that

$$\omega_{ge} = -\omega_{gi} \frac{m_e}{m_i}, \quad (4.15)$$

$$\omega_{*e} = -\omega_{*i} \frac{T_e}{T_i}, \quad (4.16)$$

$$\rho_e = -\rho_i \sqrt{\frac{m_e T_e}{m_i T_i}}, \quad (4.17)$$

equation (4.14) becomes:

$$1 + \frac{T_i}{T_e} = \frac{\omega - \omega_{gi} - \omega_{*i}}{\omega - \omega_{gi}} \left(1 - \frac{k_y^2 \rho_i^2}{2} \right) + \frac{T_i}{T_e} \frac{\omega + \frac{T_e}{T_i} \omega_{*i}}{\omega}. \quad (4.18)$$

Setting $T_i = T_e$, the result is

$$\omega^2 = -\frac{\omega_{*i} \omega_{gi}}{k_y^2 \rho_i^2 / 2} + (\omega_{gi} + \omega_{*i}) \omega + \mathcal{O}(k_y^2 \rho_i^2), \quad (4.19)$$

which is exactly the MHD result in (3.4).

We note here that the gyrokinetic dispersion relation (4.18) and the MHD dispersion relation which can be derived from (A 22) agree only up to order $\mathcal{O}(k_y \rho_i)$ and disagree at higher orders. This is the reason why we had earlier calculated our time-dependent MHD model (3.10) only up to this order.

We have confirmed that in the case of zero shear, gyrokinetics and MHD agree at least to order $\mathcal{O}(k_y \rho_i)$. This gives us a basis to presume that when the shear effects are weak, we expect there to be relatively good agreement between the two models. What remains is to derive a time-dependent gyrokinetic model with finite shear.

4.3. Finite flow shear

We now consider the full linear collisionless gyrokinetic equation (4.1) with the non-zero linear shear profile $\mathbf{u} = Sx\hat{\mathbf{y}}$. As we have done in MHD, we perform the shearing box transformation $(t, \mathbf{r}) \rightarrow (t', \mathbf{r}')$ discussed in §3.2.1 and similarly for $(t, \mathbf{R}_s) \rightarrow (t', \mathbf{R}'_s)$. The result is

$$\frac{\partial h_s}{\partial t'} + \left(w_{\parallel} \hat{\mathbf{z}} + \frac{g\hat{\mathbf{y}}}{\Omega_s} \right) \cdot \frac{\partial h_s}{\partial \mathbf{R}'_s} = \frac{Z_s e F_{0s}}{T_s} \frac{\partial \langle \delta\varphi \rangle_{\mathbf{R}}}{\partial t'} + \frac{cF_{0s}}{B} \left(\frac{d \ln n_s}{dx} + \frac{m_s g}{T_s} \right) \hat{\mathbf{y}} \cdot \frac{\partial \langle \delta\varphi \rangle_{\mathbf{R}}}{\partial \mathbf{R}'_s}. \quad (4.20)$$

We note here that we did not transform $d \ln n_s / dx$ because this is meant to be a free parameter and independent of space-time variables.

As was done in (3.8) for MHD, we consider the following solutions for the perturbed quantities

$$\delta\varphi(\mathbf{r}', t') = \widehat{\delta\varphi}(t') e^{i\mathbf{k}'_{\perp} \cdot \mathbf{r}'}, \quad (4.21)$$

$$h_s(\mathbf{R}'_s, t') = \hat{h}_s(t') e^{i\mathbf{k}'_{\perp} \cdot \mathbf{R}'_s}, \quad (4.22)$$

where we have taken $k_{\parallel} \rightarrow 0$ for flute modes. The gyroaverages are similar to (4.8) and (4.9):

$$\langle \delta\varphi \rangle_{\mathbf{R}} = \widehat{\delta\varphi}(t') e^{i\mathbf{k}'_{\perp} \cdot \mathbf{R}'_s} J_0(a_s(t'')), \quad (4.23)$$

$$\langle h_s \rangle_{\mathbf{r}} = \hat{h}_s(t') e^{i\mathbf{k}'_{\perp} \cdot \mathbf{r}'} J_0(a_s(t'')). \quad (4.24)$$

Here, we have defined:

$$a_s(t'') = \frac{w_{\perp} k_{\perp}(t')}{\Omega_s} = \frac{w_{\perp}}{\Omega_s} \sqrt{k_x^2 + k_y^2} = \frac{w_{\perp}}{\Omega_s} \sqrt{(k'_x - St'k'_y)^2 + k'_y{}^2} = \frac{w_{\perp} k'_y}{\Omega_s} \sqrt{1 + S^2 t''^2}, \quad (4.25)$$

where the origin of time has been shifted i.e. $t'' = t' - S^{-1}k'_x/k'_y$ such that for any value of k'_x , $t'' = 0$ always indicates the point where $k_x = 0$ in the lab frame. Nevertheless, as we had done in MHD, we will consider the most unstable modes with $k'_x = 0$ which means this shifting is irrelevant, but we still include it here to be consistent with the theory developed in Schekochihin *et al.* (2012).

We now rewrite the gyrokinetic system of equations (4.20) and (4.4) in terms of the new variables (t'', \mathbf{k}') , this gives us

$$\left(\frac{\partial}{\partial t} + i\omega_{gs} \right) \hat{h}_s(t) = \frac{Z_s e F_{0s}}{T_s} \left[\frac{\partial}{\partial t} + i(\omega_{gs} + \omega_{*s}) \right] J_0(a_s(t)) \widehat{\delta\varphi}(t), \quad (4.26)$$

$$\sum_s \frac{Z_s^2 e^2 n_s}{T_s} \widehat{\delta\varphi}(t) = \sum_s Z_s e \int d^3 \mathbf{w} J_0(a_s(t)) \hat{h}_s(t), \quad (4.27)$$

where the primes on all variables have been suppressed for clarity.

4.3.1. Integral equation

For finite shear, our dispersion relation takes the form of an integral equation:

$$\begin{aligned} \sum_s \frac{Z_s^2 e^2 n_s}{T_s} [1 - \Gamma_0(\lambda_s, \lambda_s)] \widehat{\delta\varphi}(t) &= \sum_s Z_s e \int d^3 \mathbf{w} J_0(a_s(t)) e^{-i\omega_{gs} t} \left[\widehat{h}_s(0) \right. \\ &\left. - \frac{Z_s e F_{0s}}{T_s} J_0(a_s(0)) \widehat{\delta\varphi}(0) \right] + \sum_s \frac{Z_s^2 e^2 n_s}{T_s} i\omega_{*s} \int_0^t d\Delta t e^{-i\omega_{gs} \Delta t} \Gamma_0(\lambda_s, \lambda'_s) \widehat{\delta\varphi}(t - \Delta t). \end{aligned} \quad (4.28)$$

The derivation of this integral equation can be found in Appendix C. Here, we have defined Γ_0 and a_s as

$$\Gamma_0(\lambda_s, \lambda'_s) = \exp\left(-\frac{\lambda_s + \lambda'_s}{2}\right) I_0\left(\sqrt{\lambda_s \lambda'_s}\right), \quad (4.29)$$

$$a_s(t) = \frac{w_\perp k_y}{\Omega_s} \sqrt{1 + S^2 t^2} = \frac{w_\perp \sqrt{2}}{v_{\text{th},s}} \sqrt{\frac{k_y^2 \rho_s^2 + S^2 t^2 k_y^2 \rho_s^2}{2}} = \frac{w_\perp}{v_{\text{th},s}} \sqrt{2\lambda_s(t)}. \quad (4.30)$$

We introduce the parameter $\lambda_s = k_\perp^2(t) \rho_i^2 / 2$ here to capture the evolution of the time-dependent wavenumber in the lab frame.

The first term on the RHS of equation (4.28) is just a source ($t = 0$) term necessary for initial value problems. It is the second term that captures the dynamics of the problem and is our focus analytically. However, when we solve (4.30) numerically later in §5, this source term will become pivotal in preventing us from obtaining a trivial solution.

4.3.2. Short-time limit

Assuming that the source terms i.e. the $t = 0$ term on the RHS of (4.28) can be neglected, we now consider the short-time regime $St \ll 1$ earlier discussed in §3.2.3. In this regime, we have $\lambda_s \approx \lambda'_s \approx \lambda_s(0) = k_y^2 \rho_s^2 / 2 \equiv \lambda_{s0}$. As a result, we have

$$\Gamma_0(\lambda_s, \lambda_s) \approx \Gamma_0(\lambda_s, \lambda'_s) \approx \Gamma_0(\lambda_{s0}, \lambda_{s0}) = I_0(\lambda_{s0}) e^{-\lambda_{s0}}. \quad (4.31)$$

The integral equation (4.28) then becomes

$$\begin{aligned} \sum_s \frac{Z_s^2 e^2 n_s}{T_s} [1 - \Gamma_0(\lambda_{s0}, \lambda_{s0})] \widehat{\delta\varphi}(t) \\ = \sum_s \frac{Z_s^2 e^2 n_s}{T_s} i\omega_{*s} \Gamma_0(\lambda_{s0}, \lambda_{s0}) \int_0^t d\Delta t e^{-i\omega_{gs} \Delta t} \widehat{\delta\varphi}(t - \Delta t). \end{aligned} \quad (4.32)$$

Since we expect the effects of shear to be weak, we can assume time-independent growth rates i.e. $\widehat{\delta\varphi}(t) \propto e^{-i\omega t}$. We then obtain

$$\sum_s \frac{Z_s^2 e^2 n_s}{T_s} [1 - \Gamma_0(\lambda_{s0}, \lambda_{s0})] = \sum_s \frac{Z_s^2 e^2 n_s}{T_s} \omega_{*s} \Gamma_0(\lambda_{s0}, \lambda_{s0}) \frac{e^{i(\omega - \omega_{gs})t} - 1}{\omega - \omega_{gs}}. \quad (4.33)$$

Splitting the complex frequency into its real and imaginary parts i.e. $\omega = \omega_R + i\gamma$. We then have $|e^{i(\omega - \omega_{gs})t}| = e^{-\gamma t}$. We shall assume a small positive growth rate $\gamma > 0$ which will be justified in a moment. Then, since our short-time limit ordering gives $t \gg 1$ (Schekochihin *et al.* 2012), this term vanishes.

For a hydrogen plasma, after using (4.31), (4.33) then becomes

$$\frac{1 - I_0(\lambda_i) e^{-\lambda_i}}{T_i} + \frac{1 - I_0(\lambda_e) e^{-\lambda_e}}{T_e} = -\frac{\omega_{*i} I_0(\lambda_i) e^{-\lambda_i}}{T_i} \frac{1}{\omega - \omega_{gi}} - \frac{\omega_{*e} I_0(\lambda_e) e^{-\lambda_e}}{T_e} \frac{1}{\omega - \omega_{ge}}, \quad (4.34)$$

by then taking the long wavelength limit $k_y \rho_i \ll 1$, the small mass ratio limit $m_e/m_i \ll 1$, and assuming that $T_i = T_e$, equation (4.34) reduces to the dispersion relation (4.14) of the zero shear case. Similar to MHD, this is expected since the effects of shear are weak in the short-time regime.

This result justifies the earlier assumption that $\gamma > 0$, since from (4.19), we know to leading order, the growth rate is simply that of the ideal MHD interchange which is positive.

4.3.3. Long time limit

In Schekochihin *et al.* (2012), a long-time limit ($St \gg 1$) asymptotic analysis for a similar integral equation was provided. Nevertheless, this analysis is difficult to replicate for the present problem due to the additional complexity of considering kinetic electrons.

To understand this, we note that based on the definition of λ_s in (4.30), we have $\lambda_e = (m_e/m_i)\lambda_i$. The short time regime is unambiguous since we will consider modes in which $k_y \rho_i \ll 1$, which we have already seen that the dispersion relations from MHD and gyrokinetics for these modes, in the case of zero shear, generally agree. Hence, the arguments of the Bessel functions $\Gamma_0(\lambda_s, \lambda_s)$ are small regardless of whether the species index s refers to the ions or electrons.

The same cannot be said for the long time limit where $St \gg 1$ and hence $\lambda_s \approx S^2 t^2 k_y^2 \rho_i^2 / 2$. In Schekochihin *et al.* (2012), this allowed for a large argument expansion of $\Gamma_0(\lambda_s, \lambda_s)$. The issue here is that even though $\lambda_i \gg 1$, it is not necessary that $\lambda_e \gg 1$ due to the presence of the factor of the mass ratio for the electrons, thereby causing the long time regime to be ambiguous.

The only definitive ‘long time regime’ is one where St is so large that $\lambda_e \gg 1$ as this automatically implies that $\lambda_i \gg 1$. Therefore there is no ambiguity when performing the large argument expansion of the Bessel functions for either species. In this scenario, we need to impose that

$$\lambda_e = \frac{m_e}{m_i} \lambda_i \gg 1. \quad (4.35)$$

Since λ_i is a measure of the time-dependent $k_\perp^2(t) \rho_i^2 / 2$ in the lab frame, so the condition (4.35) then demands that:

$$k_\perp(t) \rho_i \gg \sqrt{\frac{2m_i}{m_e}} \approx 60, \quad (4.36)$$

which is well outside the regime of interest.

Another reason why it would be difficult to formulate a long time limit asymptotic expansion for the present problem is that the analysis done in Schekochihin *et al.* (2012) requires the assumption of a single turning point for the growth rate. It will become apparent from our numerical simulations §5 that this is not an assumption we can make.

In summary, outside the short time regime, it is best to numerically integrate (4.28).

4.4. Volterra integral equation from gyrokinetics

We would now like to numerically integrate (4.28); however, as previously mentioned, we cannot neglect the source term on the RHS of the equation as this will inevitably result in the trivial solution. As this is an initial value problem, the choice of the source term will affect the final solution. As we eventually want to compare with the numerical results with GX, we shall choose the following density perturbation:

$$\hat{h}_s(0) - \frac{Z_s e F_{0s}}{T_s} J_0(a_s(0)) \widehat{\delta\varphi}(0) = \kappa F_{0s} = \kappa \frac{n_s}{\pi^{3/2} v_{\text{th},s}^3} e^{-w^2/v_{\text{th},s}^2}, \quad (4.37)$$

for some sufficiently small value of κ . This choice ensures both GX and the gyrokinetic integral equation (4.28) produce the same exponential solution when the shear is set to zero i.e. $S = 0$.

Substituting (4.37) into equation (4.28), we obtain:

$$\begin{aligned} \sum_s \frac{Z_s^2 e^2 n_s}{T_s} [1 - \Gamma_0(\lambda_s, \lambda_s)] \widehat{\delta\varphi}(t) &= \kappa \sum_s Z_s e n_s e^{-i\omega_{gs}t} e^{-\lambda_s(t)/2} \\ &+ \sum_s \frac{Z_s^2 e^2 n_s}{T_s} i\omega_{*s} \int_0^t d\Delta t e^{-i\omega_{gs}\Delta t} \Gamma_0(\lambda_s, \lambda'_s) \widehat{\delta\varphi}(t - \Delta t), \end{aligned} \quad (4.38)$$

where we have utilized the integral identity (Abramowitz & Stegun 1970):

$$\int_0^\infty e^{-a^2 t^2} t^{\nu+1} J_\nu(bt) dt = \frac{b^\nu}{(2a^2)^{\nu+1}} e^{-b^2/4a^2}. \quad (4.39)$$

For the case of a hydrogen plasma, performing the species expansion, undoing the coordinate transformation $t' \rightarrow \Delta t$ described in (C4), using the relations (4.15)–(4.17) to write everything in ionic terms, and assuming $T_i = T_e$, we finally get

$$\begin{aligned} \left[2 - \Gamma_0(\lambda_i, \lambda_i) - \Gamma_0\left(\lambda_i \frac{m_e}{m_i}, \lambda_i \frac{m_e}{m_i}\right) \right] \widehat{\delta\varphi}(t) &= \frac{\kappa T_i}{e} \left(e^{-\lambda_i/2} e^{-i\omega_{gi}t} - e^{-\lambda_i/2} \frac{m_e}{m_i} e^{i\frac{m_e}{m_i}\omega_{gi}t} \right) \\ &+ i\omega_{*i} \int_0^t dt' \left[e^{-i\omega_{gi}(t-t')} \Gamma_0(\lambda_i, \lambda'_i) - e^{i\frac{m_e}{m_i}\omega_{gi}(t-t')} \Gamma_0\left(\lambda_i \frac{m_e}{m_i}, \lambda'_i \frac{m_e}{m_i}\right) \right] \widehat{\delta\varphi}(t'), \end{aligned} \quad (4.40)$$

Self-consistently, at $t = 0$, we must have

$$\widehat{\delta\varphi}(0) = \frac{\kappa T_i}{e} \frac{e^{-\lambda_{i0}/2} - e^{-\frac{m_e}{m_i}\lambda_{i0}/2}}{2 - \Gamma_0(\lambda_{i0}, \lambda_{i0}) - \Gamma_0\left(\lambda_{i0} \frac{m_e}{m_i}, \lambda_{i0} \frac{m_e}{m_i}\right)}. \quad (4.41)$$

We now divide (4.40) throughout by $\widehat{\delta\varphi}(0)$, which gives us:

$$\begin{aligned} \frac{\widehat{\delta\varphi}(t)}{\widehat{\delta\varphi}(0)} &= \frac{e^{-\lambda_i/2} e^{-i\omega_{gi}t} - e^{-\lambda_i/2} \frac{m_e}{m_i} e^{i\frac{m_e}{m_i}\omega_{gi}t}}{e^{-\lambda_{i0}/2} - e^{-\frac{m_e}{m_i}\lambda_{i0}/2}} \frac{2 - \Gamma_0(\lambda_{i0}, \lambda_{i0}) - \Gamma_0\left(\lambda_{i0} \frac{m_e}{m_i}, \lambda_{i0} \frac{m_e}{m_i}\right)}{2 - \Gamma_0(\lambda_i, \lambda_i) - \Gamma_0\left(\lambda_i \frac{m_e}{m_i}, \lambda_i \frac{m_e}{m_i}\right)} \\ &+ i\omega_{*i} \int_0^t dt' \frac{e^{-i\omega_{gi}(t-t')} \Gamma_0(\lambda_i, \lambda'_i) - e^{i\frac{m_e}{m_i}\omega_{gi}(t-t')} \Gamma_0\left(\lambda_i \frac{m_e}{m_i}, \lambda'_i \frac{m_e}{m_i}\right)}{2 - \Gamma_0(\lambda_i, \lambda_i) - \Gamma_0\left(\lambda_i \frac{m_e}{m_i}, \lambda_i \frac{m_e}{m_i}\right)} \frac{\widehat{\delta\varphi}(t')}{\widehat{\delta\varphi}(0)}. \end{aligned} \quad (4.42)$$

This is a *Volterra equation of the second kind* (Linz 1985) in which we can solve numerically.¹ It is the solution from this equation which we hope to replicate with GX.

5. Numerical results

So far, we have derived both a MHD and gyrokinetic model for the gravitational flute interchange in §3 and §4 respectively. We would like to compare the predictions between both models as well as to hopefully get a good agreement between the gyrokinetic model and GX (Mandell *et al.* 2018, 2024); the latter would allow for the theory worked on in this paper to be used as a linear flow shear benchmark for GX. We note that we are using an alternate branch of GX that includes flow shear as well as gravity.²

¹The numerical solver used can be found here: <https://github.com/ianabel/volterra>.

²This branch of GX can be found at <https://bitbucket.org/gyrokinetics/gx/branch/gravity> and is based on <https://bitbucket.org/gyrokinetics/gx/branch/next>.

5.1. GX Normalizations

To make direct comparisons with GX, it is convenient for us to normalize both the MHD and gyrokinetic equations for the case of zero shear i.e. (3.5) and (4.13), and the case of finite shear i.e. (3.10) and (4.42). We shall follow the normalizations found in Appendix A of Mandell *et al.* (2024). We note here that this reference follows a different convention in the definition of $v_{\text{th},s}$ (and hence ρ_s) in which the factor of $\sqrt{2}$ is absent. Nevertheless, our derived equations can be easily modified to include this factor. From this point on, for any quantity α , we shall denote its corresponding GX normalized quantity by a tilde above i.e. $\tilde{\alpha}$.

In the case of zero shear, the normalized MHD (3.5) and gyrokinetic (4.13) dispersion relations are:

$$\tilde{\omega} - \frac{1}{2} \left[(\tilde{\omega}_{gi} + \tilde{\omega}_{*i}) \pm \sqrt{(\tilde{\omega}_{gi} + \tilde{\omega}_{*i})^2 - 4 \frac{\tilde{\omega}_{gi}\tilde{\omega}_{*i}}{\tilde{k}_y^2}} \right] = 0, \quad (5.1)$$

$$2 - \frac{\tilde{\omega} - \tilde{\omega}_{gi} - \tilde{\omega}_{*i}}{\tilde{\omega} - \tilde{\omega}_{gi}} I_0(\tilde{k}_y^2) e^{-\tilde{k}_y^2} + \frac{\tilde{\omega} + \tilde{m}_e \tilde{\omega}_{gi} + \tilde{\omega}_{*i}}{\tilde{\omega} + \tilde{m}_e \tilde{\omega}_{gi}} I_0(\tilde{m}_e \tilde{k}_y^2) e^{-\tilde{m}_e \tilde{k}_y^2} = 0. \quad (5.2)$$

In the case of finite shear, the time-dependent MHD (3.10) and gyrokinetic (4.42) equations are:

$$\left\{ \frac{\partial^2}{\partial \tilde{t}^2} + \left[\frac{2\tilde{S}^2 \tilde{t}}{\tilde{S}^2 \tilde{t}^2 + 1} - i(\tilde{\omega}_{gi} + \tilde{\omega}_{*i}) \right] \frac{\partial}{\partial \tilde{t}} - \frac{i\tilde{S}^2 \tilde{t} (2\tilde{\omega}_{gi} + \tilde{\omega}_{*i}) + \tilde{\omega}_{gi}\tilde{\omega}_{*i}/\tilde{k}_y^2}{\tilde{S}^2 \tilde{t}^2 + 1} \right\} \frac{\tilde{\delta n}_i(\tilde{t})}{\tilde{\delta n}_i(0)} = 0, \quad (5.3)$$

and

$$\begin{aligned} \frac{\tilde{\delta \varphi}(\tilde{t})}{\tilde{\delta \varphi}(0)} &= \frac{e^{-\lambda_i/2} e^{-i\tilde{\omega}_{gi}\tilde{t}} - e^{-\tilde{m}_e \lambda_i/2} e^{i\tilde{m}_e \tilde{\omega}_{gi}\tilde{t}}}{e^{-\lambda_{i0}/2} - e^{-\tilde{m}_e \lambda_{i0}/2}} \frac{2 - \Gamma_0(\lambda_{i0}, \lambda_{i0}) - \Gamma_0(\tilde{m}_e \lambda_{i0}, \tilde{m}_e \lambda_{i0})}{2 - \Gamma_0(\lambda_i, \lambda_i) - \Gamma_0(\tilde{m}_e \lambda_i, \tilde{m}_e \lambda_i)} \\ &+ i\tilde{\omega}_{*i} \int_0^{\tilde{t}} d\tilde{t}' \frac{e^{-i\tilde{\omega}_{gi}(\tilde{t}-\tilde{t}')} \Gamma_0(\lambda_i, \lambda'_i) - e^{i\tilde{m}_e \tilde{\omega}_{gi}(\tilde{t}-\tilde{t}')} \Gamma_0(\tilde{m}_e \lambda_i, \tilde{m}_e \lambda'_i)}{2 - \Gamma_0(\lambda_i, \lambda_i) - \Gamma_0(\tilde{m}_e \lambda_i, \tilde{m}_e \lambda_i)} \frac{\tilde{\delta \varphi}(\tilde{t}')}{\tilde{\delta \varphi}(0)}. \end{aligned} \quad (5.4)$$

Note that, in (5.4), using the definition (4.30), we have $\lambda_i(\tilde{t}) = \tilde{k}_y^2 (1 + \tilde{S}^2 \tilde{t}^2)$.

In the equations (5.1)–(5.4), the free parameters are given by $\{\tilde{\omega}_{gi}, \tilde{\omega}_{*i}, \tilde{k}_y, \tilde{S}\}$. However, the input parameters in GX are $\{\tilde{g}, f_{\text{prim}}, \tilde{k}_y, \tilde{S}\}$ where \tilde{g} is the normalized gravity and f_{prim} is the normalized density gradient. These two sets of free parameters are related by

$$\tilde{\omega}_{gi} = \tilde{g} \tilde{k}_y, \quad (5.5)$$

and

$$\tilde{\omega}_{*i} = \tilde{k}_y f_{\text{prim}}. \quad (5.6)$$

5.2. Gyrokinetic perturbed density

For finite shear, we note that the gyrokinetic integral equation (5.4) solves for $\tilde{\delta \varphi}/\tilde{\delta \varphi}(0)$ while the MHD equation (5.3) solves for $\tilde{\delta n}_i/\tilde{\delta n}_i(0)$. We therefore need to find a way to solve for $\tilde{\delta n}_i/\tilde{\delta n}_i(0)$ in the former. In Appendix D, we demonstrate how this can be

achieved by using our earlier solution for $\hat{h}_i(t)$ to compute $\widehat{\delta n}_i(t)$ from $\widehat{\delta\varphi}(t)$. After which, applying the GX normalizations would give us $\widetilde{\delta n}_i$. The result is:

$$\frac{\widetilde{\delta n}_i}{\widetilde{\delta n}_i(0)} = i\tilde{\omega}_{*i} \int_0^{\tilde{t}} d\tilde{t}' \frac{e^{-i\tilde{\omega}_{gi}(\tilde{t}-\tilde{t}')} \Gamma_0(\lambda_i, \lambda'_i)}{\alpha_0} \frac{\widetilde{\delta\varphi}(\tilde{t}')}{\widetilde{\delta\varphi}(0)} + \frac{1}{\alpha_0} \left\{ [\Gamma_0(\lambda_i, \lambda_i) - 1] \frac{\widetilde{\delta\varphi}}{\widetilde{\delta\varphi}(0)} + e^{-i\tilde{\omega}_{gi}\tilde{t}} e^{-\lambda_i/2} \frac{2 - \Gamma_0(\lambda_{i0}, \lambda_{i0}) - \Gamma_0(\tilde{m}_e \lambda_{i0}, \tilde{m}_e \lambda_{i0})}{e^{-\lambda_{i0}/2} - e^{-\tilde{m}_e \lambda_{i0}/2}} \right\}, \quad (5.7)$$

where

$$\alpha_0 = e^{-\lambda_{i0}/2} \frac{2 - \Gamma_0(\lambda_{i0}, \lambda_{i0}) - \Gamma_0(\tilde{m}_e \lambda_{i0}, \tilde{m}_e \lambda_{i0})}{e^{-\lambda_{i0}/2} - e^{-\tilde{m}_e \lambda_{i0}/2}} + [\Gamma_0(\lambda_{i0}, \lambda_{i0}) - 1]. \quad (5.8)$$

In other words, once (5.4) is solved, the solution must be inserted into (5.7). The time-integral can then be evaluated by numerical integration where we have opted for the trapezoidal rule. This result is then the correct quantity to be compared with MHD. In Appendix D we will also explain how to obtain this quantity from GX.

5.3. Influence of initial conditions

In order to choose appropriate values for the free parameters $\tilde{\omega}_{gi}$ and $\tilde{\omega}_{*i}$, we will need to analyse the structure of the (finite shear) equations. In particular, the source term in the gyrokinetic integral equation (5.4) is of considerable interest, which we recall is a consequence of the choice of an initial density perturbation (4.37).

Firstly, we note that this source term is the only term that does not contain the perturbation ratio $\widetilde{\delta\varphi}/\widetilde{\delta\varphi}(0)$ in the integral equation (5.4). On the other hand, no such term exists in the MHD equation (5.3) as all terms are multiplied by $\widetilde{\delta n}_i/\widetilde{\delta n}_i(0)$. While it is possible to capture the same initial conditions in the MHD model via the initial value of its derivative (see Appendix E), we should not expect the time evolution of this source term to be fully captured. This boils down to the fact that, even though we have set (4.37) as a condition on \hat{h}_s , from (4.7), we see that $h_s(0) \propto e^{ik_y \mathbf{R}_s} \hat{\mathbf{y}}$. Physically, this means that finite FLR effects are embedded into the initial conditions of the gyrokinetic solution and the MHD model cannot hope to fully capture it as it only contains FLR effects to first order. This leads to a natural divergence, which we will later demonstrate in our numerics when source term effects are strong.

Secondly, we would like to determine when the source term is dominant. This is important because we recall from our prior derivations that both the gyrokinetic integral equation and MHD equation arrive at the same dispersion relation (4.19) in the short-time limit $St \ll 1$ provided that the source-term is neglected in the former. This implies that the main FLR physics is in fact captured solely by the integral term of (5.4). Since it is the only term multiplied by $\tilde{\omega}_{*i}$, a simple way we can make it dominant is by choosing $\tilde{\omega}_{*i}$ to be sufficiently large. In our numerics, we shall illustrate two case $f_{\text{prim}} = 0.5$ and $f_{\text{prim}} = 15$ where the former is termed the *strong source regime* and the latter is termed the *weak source regime*.

Thirdly, we note that the parameter $\tilde{\omega}_{gi}$ is tied to oscillatory terms in (5.4). Therefore, to avoid significant oscillation, we choose a ‘safe’ value of $\tilde{g} = 0.05$. In addition, if we compare our MHD equation (3.10) to that of Ng & Hassam (2005) given in (B3), we observe that the difference between these two equations are solely due to the terms multiplied by a factor of $\tilde{\omega}_{gi}$. Therefore, by choosing \tilde{g} and hence $\tilde{\omega}_{gi}$ to be small, we can ensure that the solutions from both MHD models are numerically similar.

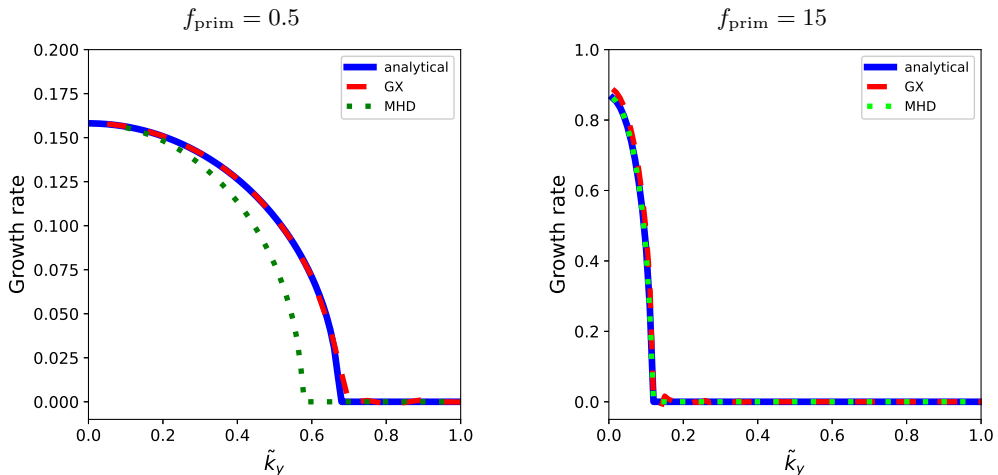


FIGURE 3: Plot of the growth rate $\Im\{\omega\}$ against \tilde{k}_y computed from MHD (5.1), gyrokinetics (5.2), and GX. The left panel represents the strong source regime while the right panel represents the weak source regime.

5.4. Zero flow shear

We first compare the linear growth rates predicted by MHD, gyrokinetics, and GX in the case of zero shear. This is depicted in Figure 3 and is evident the unstable modes are those for which $\tilde{k}_y \ll 1$. In the case of finite shear, the shear pushes \tilde{k}_\perp (equivalently \tilde{k}_y for zero shear) higher and higher until these unstable modes reaches the FLR stabilization threshold, beyond which we expect a decaying solution. Therefore, by comparing the prediction of this threshold value by these different models, we would be able to get some sense of when the decay should be observed.

In the strong source regime, we see that MHD predicts the FLR stabilization threshold to be $\tilde{k}_\perp = \tilde{k}_y \approx 0.575$ while gyrokinetics predicts it to be $\tilde{k}_\perp = \tilde{k}_y \approx 0.674$. Later on, for finite shear, since $\tilde{k}_\perp^2 = \lambda_i(\tilde{t}) = \tilde{k}_y^2(1 + \tilde{S}^2\tilde{t}^2)$, we expect a decay at:

$$\tilde{t}_{\text{FLR,MHD}} \approx \sqrt{\frac{1}{\tilde{S}^2} \left(\frac{0.575^2}{\tilde{k}_y^2} - 1 \right)}, \quad (5.9)$$

$$\tilde{t}_{\text{FLR,GK}} \approx \sqrt{\frac{1}{\tilde{S}^2} \left(\frac{0.674^2}{\tilde{k}_y^2} - 1 \right)}. \quad (5.10)$$

In the weak source regime, both MHD and gyrokinetics predict the same FLR stabilization threshold to be $\tilde{k}_\perp = \tilde{k}_y \approx 0.115$. Hence, for finite shear, the approximate time a decay solution is expected is:

$$\tilde{t}_{\text{FLR,MHD}} = \tilde{t}_{\text{FLR,GK}} \approx \sqrt{\frac{1}{\tilde{S}^2} \left(\frac{0.115^2}{\tilde{k}_y^2} - 1 \right)}. \quad (5.11)$$

It is particularly interesting to note that even though the instability is stronger in the weak source regime due to a larger f_{prim} , the FLR stabilization threshold wavenumber is smaller compared to that of the strong source regime. This seems to suggest that the

shear would be *more effective* for more unstable modes, forcing them to reach a decay solution earlier. We will indeed later observe this in our numerical simulations.

5.5. Finite flow shear

We now turn our attention to the time traces of the ratio to the initial perturbation predicted by MHD (5.3) and gyrokinetics (5.7) in the presence of flow shear. Before discussing the numerical results, we first like to describe a few parameters that one should pay some attention to when running these simulations in GX.

5.5.1. GX inputs for box size and number of modes in the x direction

The maximum time that our flow shear simulation can run in GX is controlled by the following input parameters: the shear strength \tilde{S} , the number of Fourier modes in \tilde{k}_x which we shall denote by N_{kx} , and the box size in x which we shall denote by \tilde{x}_0 . To understand this dependence, we note that N_{kx} sets both the number of positive and negative \tilde{k}_x modes, symmetric about zero. On the other hand, the \tilde{k}_x interval is determined by $\Delta\tilde{k}_x = 1/\tilde{x}_0$. This sets the (absolute) maximum \tilde{k}_x in the system to be $\tilde{k}_{x,\max} = \Delta\tilde{k}_x(N_{kx} - 1)/2$. As \tilde{k}_x is increasing with time in our problem as seen in (3.9), we can calculate when $|\tilde{k}_x(t)|$ reaches $\tilde{k}_{x,\max}$, beyond which it falls off the grid:

$$|\tilde{k}_{x,\max}(\tilde{t}_{\max})| = \tilde{S}\tilde{t}_{\max}\tilde{k}_y \implies \tilde{t}_{\max} = \frac{\Delta\tilde{k}_x N_{kx} - 1}{\tilde{S}\tilde{k}_y} = \frac{N_{kx} - 1}{2\tilde{x}_0\tilde{S}\tilde{k}_y}. \quad (5.12)$$

This is important for two reasons. Firstly, for when analyzing scenarios with strong flow shear, one needs either a large N_{kx} or a small \tilde{x}_0 to allow the simulation to run for a reasonable amount of time. Secondly, our numerical tests reveal that choosing too small a value of \tilde{x}_0 would result in unphysical discontinuities in the solution. Therefore, some care must be taken when choosing the inputs N_{kx} and \tilde{x}_0 .

We will work with $\tilde{x}_0 = 256.0$ in our flow shear simulations and use $N_{kx} = 2^{15}$. An exception to this is the weak shear scenario for the strong source regime where a longer simulation time is required to demonstrate the decay, imploring us to use $N_{kx} = 2^{16}$.

GX is a parallelized code with a Fourier decomposition in (perpendicular) configuration space and Hermite-Laguerre decomposition for velocities (Mandell *et al.* 2018, 2024). It works with with a maximum of 1 GPU per species per Hermite moment; therefore, as these simulations used 8 Hermite moments and 2 kinetic species, 4 Perlmutter nodes with 4 GPUs per node was utilized.¹

5.5.2. Observations for increasing flow shear

Our flow shear results are shown in Figure 4. We first discuss the strong source regime on the left column. As expected, both gyrokinetics and MHD predict that an increased shear results in a suppression of the transient amplification, with their solutions diverging at $\tilde{k}_\perp = 1$ as MHD inherently assumes that $\tilde{k}_\perp \ll 1$. However, the fact that the FLR stabilization for gyrokinetics takes place at a much later time compared to that of MHD may appear contradictory to what was obtained for the zero shear result (5.9) and (5.10). In reality, this should not be surprising because the gyrokinetic equation used to derive the zero shear result (5.2) relied on the assumption that the source term was negligible (see §4.3.2), which is clearly not the case in the strong source regime. Another issue depicted is that in the case of weak shear, the GX solution seems to predict an eventual exponential growing solution. This is likely due to the long time runs of these simulations,

¹Perlmutter is the high performance computing facility at the National Energy Research Scientific Computing Center.

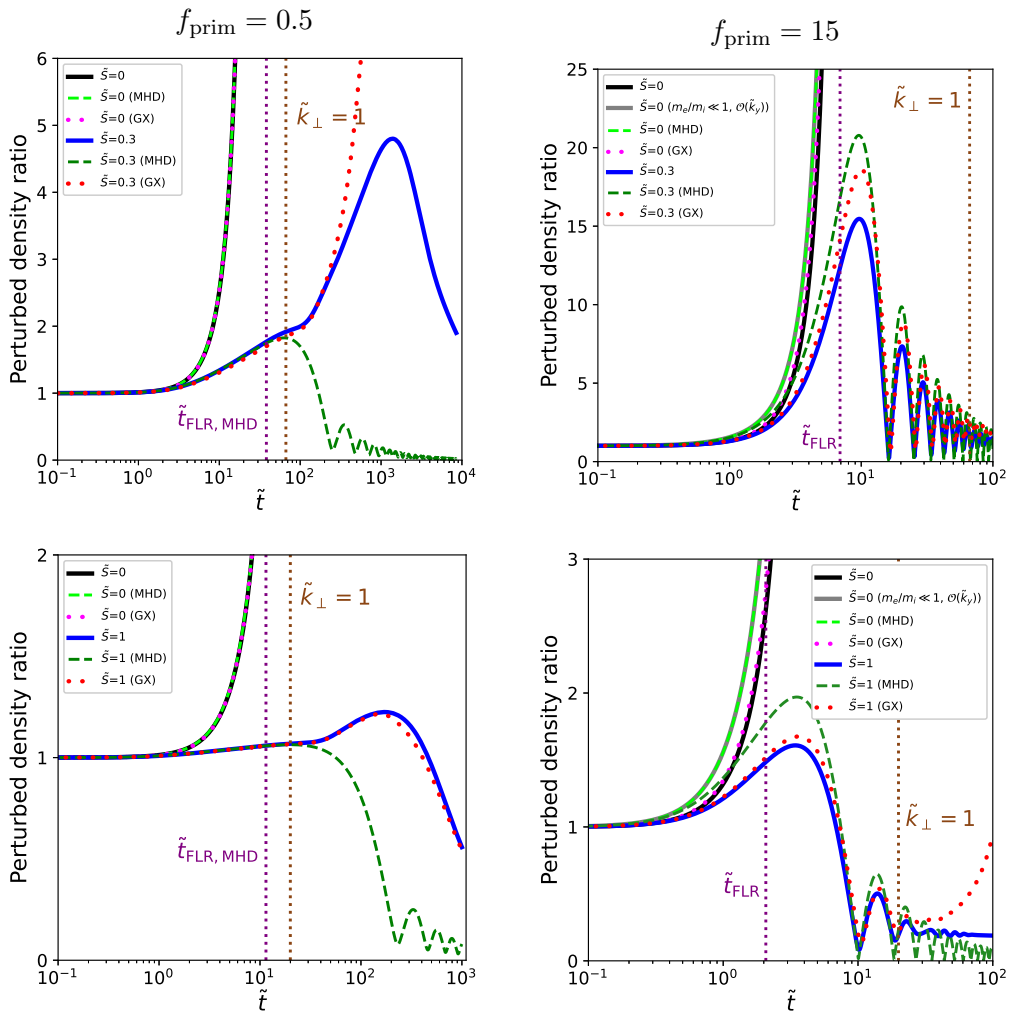


FIGURE 4: Plots of $\tilde{\delta n}_i / \tilde{\delta n}_i(0)$ against \tilde{t} . The left column represents the strong source regime $f_{\text{prim}} = 0.5$ in the case of weak shear ($\tilde{S} = 0.3$) and strong shear ($\tilde{S} = 1$). This is the same for weak source regime $f_{\text{prim}} = 15$ on the right column. The solid lines (black, blue, grey) represent solutions computed analytically from (5.7) and (5.4). The dashed lines (lime, green) are from the MHD equation (5.3). The dots (pink, red) are the solutions from GX. The vertical dotted purple line represents the supposed time in which FLR stabilization, as predicted by MHD, is expected to occur, calculated from (5.9) and (5.11) for the left and right columns respectively. The vertical dotted brown line represents the time for which $\tilde{k}_{\perp} = 1$, the point at which MHD and gyrokinetics are expected to diverge. In each figure, the $\tilde{S} = 0$ solution for each model is always presented as a reference.

which we have observed to cause an eventual inversion of the Laguerre spectra used in GX, possibly due to finite precision errors.

On the other hand, for the weak source regime on the right column where the FLR physics dominate, we see that both gyrokinetics and MHD agree on the FLR stabilization time. Moreover, despite the instability being much stronger, we see that the shear is more effective, ensuring a decay solution is reached more quickly. Both these results agree with

our expectations from the zero shear scenario. It is interesting to note that despite the FLR stabilization occurring at times much earlier than $\tilde{k}_\perp = 1$, the MHD solution appears to underestimate the effects of shear in the sense that the maximal amplification is much larger than that of gyrokinetics. This can be attributed to the fact that even at zero shear, there are small deviations between the gyrokinetic and MHD solutions, resolved only by taking the $m_e/m_i \ll 1$ and $\tilde{k}_y \ll 1$ limit of the former, for which the details are left to Appendix F.

6. Conclusion and future work

This paper presents two models, one based on isothermal compressible MHD inspired by Roberts & Taylor (1962) and Ng & Hassam (2005) as well as another based on gyrokinetics in an attempt to describe flow shear induced FLR stabilization of flute interchanges in slab geometry.

At zero shear, in contrast to ideal MHD where all modes are predicted to be unstable, we demonstrated that by including FLR effects, which is inherent in gyrokinetics and achieved in MHD by adding gyroviscosity, there exists a threshold value of $k_\perp \rho_i$ beyond which all modes are stable. This is known as FLR stabilization and we have numerically shown that gyrokinetics and MHD predict similar values of this threshold.

When the shear becomes finite, it causes an initially unstable mode with $k_\perp \rho_i \ll 1$ to eventually become stable by ‘tilting’ the mode, thereby increasing $k_\perp \rho_i$ until it crosses the aforementioned threshold. However, in the time before FLR stabilization occurs, there can be transient amplification of this unstable mode. Due to the nature of the derived gyrokinetic integral equation, the initial conditions result in a time-dependent source term. Therefore, the numerical simulations were carried out in two regimes depending on whether this source is strong or weak.

In the strong source regime, the influence of the source results in the FLR stabilization for the gyrokinetic solution taking place at a much later time, in contrast with what was expected from the zero shear scenario. The MHD and gyrokinetic solutions were found to deviate at $k_\perp \rho_i \sim 1$ which is expected on account of the long wavelength assumption in MHD.

In the weak source regime where the FLR physics is dominant, both the gyrokinetic and MHD solution predicts the same FLR stabilization time, consistent with the result from our zero shear scenario. However, we have observed that MHD seems to underestimate the effects of shear as compared to gyrokinetics.

The results from both regimes demonstrate that the transient amplification of the unstable mode is suppressed with increasing shear. Moreover, it shows that the shear appears to be more effective for more unstable modes, causing them to reach a decay solution faster.

We now discuss some potential extensions to the work at hand. To begin with, we note that we have focused mainly on electrostatic perturbations. As explained in the introduction, we have done so because it is the fluctuating electric field that is responsible for driving the instability. Regardless, it is entirely possible to include a perturbed magnetic field to this problem and consider full electromagnetic effects.

We had also chosen to focus on the the flute modes ($k_\parallel \rightarrow 0$) as they are the most unstable. However, the above analysis can be extended to include finite k_\parallel effects in the manner similar to Schekochihin *et al.* (2012). It would be interesting to compare the shear stabilization of these modes with the flute modes.

Another feature that this work did not include is that of collisions. As already mentioned, we had neglected this because we are utilizing previously derived collisionless

models as our base of comparison. Despite this, we should note that the linearized collision operators used in gyrokinetics contains terms that are proportional to $k_{\perp}^2 \rho_i^2$ (Abel *et al.* 2008). Hence, these terms may potentially be significant as $k_{\perp} \rho_i \rightarrow 1$, making it valuable to understand their role in the problem in the future.

7. Acknowledgements

We express our gratitude to M. Landreman and the stellarator group at the University of Maryland, College Park for the insightful discussions.

This research used resources of the National Energy Research Scientific Computing Center (NERSC), a Department of Energy User Facility using NERSC award FES-ERCAP 36155.

This material is based upon work supported by the U.S. Department of Energy, Office of Science, Office of Fusion Energy Sciences, through the SciDAC program under Award Number DE-SC0024425 and Award Number DEFG0293ER54197.

8. Declaration of Interests

Dr Ian Abel is the co-founder of Gridfire Inc. a company engaged in the commercialization of the centrifugal mirror concept.

Appendix A. Derivation of the extended MHD model with gyroviscosity

A.1. Extended MHD equations

The extended MHD equations found in Roberts & Taylor (1962) comprises the following equations:

$$\text{Momentum: } m_i N_i \left(\frac{\partial}{\partial t} + \mathbf{U} \cdot \nabla \right) \mathbf{U} = -\nabla(p_i + p_e) + m_i N_i \mathbf{g} + \nu_i \boldsymbol{\lambda}_i, \quad (\text{A } 1)$$

$$\text{Continuity: } \frac{\partial N_i}{\partial t} + \nabla \cdot (N_i \mathbf{U}) = 0, \quad (\text{A } 2)$$

$$\text{Ohm's law: } \mathbf{E} + \mathbf{U} \times \mathbf{B} + \frac{c}{e N_i} \nabla p_e = 0, \quad (\text{A } 3)$$

where we have neglected electron inertia and electron gyroviscosity. The capital letter quantities N_i, \mathbf{U}_i consists of both the equilibrium quantity and its perturbation ($N_i = n_i + \delta n_i$ and $\mathbf{U}_i = Sx\hat{\mathbf{y}} + \delta\mathbf{u}$). Also, we have $\nu_i = \rho_i^2 \Omega_i / 4$ and

$$\lambda_x = m_i \frac{\partial}{\partial x} \left[N_i \left(\frac{\partial U_y}{\partial x} + \frac{\partial U_x}{\partial y} \right) \right] - m_i \frac{\partial}{\partial y} \left[N_i \left(\frac{\partial U_x}{\partial x} - \frac{\partial U_y}{\partial y} \right) \right], \quad (\text{A } 4)$$

$$\lambda_y = -m_i \frac{\partial}{\partial y} \left[N_i \left(\frac{\partial U_y}{\partial x} + \frac{\partial U_x}{\partial y} \right) \right] - m_i \frac{\partial}{\partial x} \left[N_i \left(\frac{\partial U_x}{\partial x} - \frac{\partial U_y}{\partial y} \right) \right], \quad (\text{A } 5)$$

where the quantity $\boldsymbol{\lambda}$ is simply equivalent to $-\nabla \cdot \mathbf{\Pi}_{i \times}$ where $\mathbf{\Pi}_{i \times}$ is the gyro-viscosity component of the Braginskii stress tensor (Braginskii 1965; Schnack *et al.* 2006; Parra 2019). We will also assume our MHD model to have isothermal ions i.e. $p_i = n_i T_i$ with $T_i = \text{constant}$, as was done in Ng & Hassam (2005).

It is convenient to substitute the momentum equation (A 1) as an expression for p_e in

(A 3). This gives us

$$\mathbf{E} + \mathbf{U} \times \mathbf{B} - \frac{c}{en} \nabla p_i - \frac{m_i c}{e} \left(\frac{\partial}{\partial t} + \mathbf{U} \cdot \nabla \right) \mathbf{U} + \frac{m_i c}{e} \mathbf{g} + \frac{c}{e} \frac{\nu_i}{N_i} \boldsymbol{\lambda} = 0. \quad (\text{A } 6)$$

Taking the curl of this equation and utilizing Faraday's law $c \nabla \times \mathbf{E} = \partial_t \mathbf{B} = 0$, we obtain

$$\hat{z} \nabla \cdot \mathbf{U} + \frac{1}{\Omega_i} \nabla \times \left(\frac{\partial}{\partial t} + \mathbf{U} \cdot \nabla \right) \mathbf{U} - \frac{\nu_i}{m_i \Omega_i} \nabla \times \left(\frac{1}{N_i} \boldsymbol{\lambda}_i \right) = 0. \quad (\text{A } 7)$$

Equations (A 1), (A 2), and (A 7) are our extended MHD equations

A.2. Linearization of extended MHD equations

A.2.1. Ordering assumptions

We want to linearize the extended MHD equations (A 1), (A 2), and (A 7). However, because the linearized equations are too complicated for our purposes, we will take inspiration from the gyrokinetic ordering (Abel *et al.* 2013) to neglect certain small terms. We shall assume that

$$\frac{\partial}{\partial t} \sim \omega \sim \epsilon \Omega_i, \quad \rho_i \sim \epsilon a, \quad \frac{\partial}{\partial x} \sim \frac{\partial}{\partial y} \sim k_{\perp} \sim \frac{1}{\rho_i}, \quad \frac{n'_i}{n_i} \sim \frac{1}{a}, \quad (\text{A } 8)$$

where we note that $k_{\perp} \rho_i \ll 1$ comes as a subsidiary expansion (Schekochihin *et al.* 2009).

We need to come up with the ordering assumptions for S , δu_x , δu_y , and δn_i . We assume $\delta n_i \sim \epsilon n_i$ and $\delta u_x \sim \delta u_y \sim \epsilon v_{\text{th},i}$. For S , we are interested in the regime where

$$S \sim \gamma_g \sim \frac{v_{\text{th},i}}{a} \sim \omega, \quad (\text{A } 9)$$

where γ_g is the ideal interchange growth rate given in (3.1).

A.2.2. Linearized equations

Firstly, for the momentum equation (A 1), we take the curl, linearize it, and divide throughout by n_i . In the flute limit $k_{\parallel} \rightarrow 0$, we obtain

$$\begin{aligned} & \underbrace{\frac{\partial}{\partial t}}_{\sim \epsilon \Omega_i} \left[\underbrace{\left(\frac{\partial \delta u_y}{\partial x} - \frac{\partial \delta u_x}{\partial y} \right)}_{\sim \epsilon \Omega_i} + \underbrace{\frac{n'_i}{n_i} \delta u_y}_{\sim \epsilon^2 \Omega_i} \right] + \underbrace{S}_{\sim \epsilon \Omega_i} \left[\underbrace{\frac{n'_i}{n_i} \left(\delta u_x + x \frac{\partial \delta u_y}{\partial y} \right)}_{\sim \epsilon^2 \Omega_i} \right. \\ & \left. + \underbrace{\frac{\partial \delta u_x}{\partial x} + \frac{\partial \delta u_y}{\partial y} + x \frac{\partial^2 \delta u_y}{\partial x \partial y} - x \frac{\partial^2 \delta u_x}{\partial y^2}}_{\sim \epsilon \Omega_i} \right] \\ & = \underbrace{g \frac{\partial}{\partial y} \left(\frac{\delta n_i}{n_i} \right)}_{\sim \epsilon^2 \Omega_i^2} + \underbrace{\nu_i}_{\sim \epsilon^2 a^2 \Omega_i} \left\{ \underbrace{- \frac{n''_i}{n_i} \left(\frac{\partial \delta u_x}{\partial x} - \frac{\partial \delta u_y}{\partial y} \right)}_{\sim \epsilon \Omega_i / a^2} - \underbrace{2 \frac{n'_i}{n_i} \left(\frac{\partial^2 \delta u_x}{\partial x^2} + \frac{\partial^2 \delta u_x}{\partial y^2} \right)}_{\sim \Omega_i / a^2} \right. \\ & \left. - \underbrace{\frac{\partial^3 \delta u_y}{\partial y \partial x^2} - \frac{\partial^3 \delta u_x}{\partial y^2 \partial x} - \frac{\partial^3 \delta u_x}{\partial x^3} - \frac{\partial^3 \delta u_y}{\partial y^3}}_{\sim \Omega_i / \epsilon a^2} - \underbrace{2S \frac{\partial^2}{\partial x \partial y} \left(\frac{\delta n_i}{n_i} \right)}_{\sim \Omega_i / a^2} \right\}. \quad (\text{A } 10) \end{aligned}$$

We only retain terms that are comparable in size to the lowest non-vanishing time-derivative on the LHS; therefore, we retain only up to $\mathcal{O}(\epsilon^2)$ and the equation reduces

to

$$\begin{aligned} & \left(\frac{\partial}{\partial t} + Sx \frac{\partial}{\partial y} \right) \left(\frac{\partial \delta u_y}{\partial x} - \frac{\partial \delta u_x}{\partial y} \right) + S \left(\frac{\partial \delta u_x}{\partial x} + \frac{\partial \delta u_y}{\partial y} \right) = g \frac{\partial}{\partial y} \left(\frac{\delta n_i}{n_i} \right) \\ & + \nu_i \left[-2 \frac{n'_i}{n_i} \left(\frac{\partial^2 \delta u_x}{\partial x^2} + \frac{\partial^2 \delta u_x}{\partial y^2} \right) - \frac{\partial^3 \delta u_y}{\partial y \partial x^2} - \frac{\partial^3 \delta u_x}{\partial y^2 \partial x} - \frac{\partial^3 \delta u_x}{\partial x^3} - \frac{\partial^3 \delta u_y}{\partial y^3} \right. \\ & \left. - 2S \frac{\partial^2}{\partial x \partial y} \left(\frac{\delta n_i}{n_i} \right) \right]. \end{aligned} \quad (\text{A } 11)$$

Next, for the continuity equation (A 2), we linearize and divide throughout by n_i :

$$\left(\frac{\partial}{\partial t} + Sx \frac{\partial}{\partial y} \right) \frac{\delta n_i}{n_i} + \left(\frac{\partial \delta u_x}{\partial x} + \frac{\partial \delta u_y}{\partial y} \right) + \frac{n'_i}{n_i} \delta u_x = 0. \quad (\text{A } 12)$$

No ordering approximations are required here since all terms are $\mathcal{O}(\epsilon)$ or larger.

Lastly, for Ohm's law (A 7), we take the dot product with \hat{z} and linearize:

$$\begin{aligned} & \underbrace{\frac{\partial \delta u_x}{\partial x} + \frac{\partial \delta u_y}{\partial y}}_{\sim \epsilon \Omega_i} + \frac{1}{\Omega_i} \left[\underbrace{\left(\frac{\partial}{\partial t} + Sx \frac{\partial}{\partial y} \right)}_{\sim \epsilon \Omega_i} \underbrace{\left(\frac{\partial \delta u_y}{\partial x} - \frac{\partial \delta u_x}{\partial y} \right)}_{\sim \epsilon \Omega_i} + S \underbrace{\left(\frac{\partial \delta u_x}{\partial x} + \frac{\partial \delta u_y}{\partial y} \right)}_{\sim \epsilon^2 \Omega_i^2} \right] \\ & + \underbrace{\frac{\nu_i}{\Omega_i}}_{\sim \epsilon^2 a^2} \left\{ \underbrace{\frac{n''_i}{n_i} \left(\frac{\partial \delta u_x}{\partial x} - \frac{\partial \delta u_y}{\partial y} \right) - \left(\frac{n'_i}{n_i} \right)^2 \left(\frac{\partial \delta u_x}{\partial x} - \frac{\partial \delta u_y}{\partial y} \right) + \frac{n'_i}{n_i} \left(\frac{\partial^2 \delta u_x}{\partial x^2} + \frac{\partial^2 \delta u_x}{\partial y^2} \right)}_{\sim \epsilon \Omega_i / a^2} \right. \\ & \quad \left. - 2S \frac{n'_i}{n_i} \frac{\partial}{\partial y} \left(\frac{\delta n_i}{n_i} \right) + \underbrace{\frac{\partial^3 \delta u_y}{\partial y \partial x^2} + \frac{\partial^3 \delta u_x}{\partial y^2 \partial x} + \frac{\partial^3 \delta u_x}{\partial x^3} + \frac{\partial^3 \delta u_y}{\partial y^3}}_{\sim \Omega_i / \epsilon a^2} \right. \\ & \quad \left. + 2S \frac{\partial^2}{\partial x \partial y} \left(\frac{\delta n_i}{n_i} \right) \right\}_{\sim \Omega_i / a^2} \\ & = 0. \end{aligned} \quad (\text{A } 13)$$

Again, retaining up to only $\mathcal{O}(\epsilon^2)$, we obtain

$$\begin{aligned} & \frac{\partial \delta u_x}{\partial x} + \frac{\partial \delta u_y}{\partial y} + \frac{1}{\Omega_i} \left[\left(\frac{\partial}{\partial t} + Sx \frac{\partial}{\partial y} \right) \left(\frac{\partial \delta u_y}{\partial x} - \frac{\partial \delta u_x}{\partial y} \right) + S \left(\frac{\partial \delta u_x}{\partial x} + \frac{\partial \delta u_y}{\partial y} \right) \right] \\ & + \frac{\nu_i}{\Omega_i} \left[\frac{n'_i}{n_i} \left(\frac{\partial^2 \delta u_x}{\partial x^2} + \frac{\partial^2 \delta u_x}{\partial y^2} \right) + \frac{\partial^3 \delta u_y}{\partial y \partial x^2} + \frac{\partial^3 \delta u_x}{\partial y^2 \partial x} + \frac{\partial^3 \delta u_x}{\partial x^3} + \frac{\partial^3 \delta u_y}{\partial y^3} + 2S \frac{\partial^2}{\partial x \partial y} \left(\frac{\delta n_i}{n_i} \right) \right] \\ & = 0. \end{aligned} \quad (\text{A } 14)$$

The three equations (A 11), (A 12), and (A 14) are the linearized equations that solve for the three unknowns δn_i , δu_x , and δu_y .

A.3. Zero shear dispersion relation

In the case of zero shear ($S = 0$), the three equations become

$$\begin{aligned} \frac{\partial}{\partial t} \left(\frac{\partial \delta u_y}{\partial x} - \frac{\partial \delta u_x}{\partial y} \right) &= g \frac{\partial}{\partial y} \left(\frac{\delta n_i}{n_i} \right) + \nu_i \left[-2 \frac{n'_i}{n_i} \left(\frac{\partial^2 \delta u_x}{\partial x^2} + \frac{\partial^2 \delta u_x}{\partial y^2} \right) \right. \\ &\quad \left. - \frac{\partial^3 \delta u_y}{\partial y \partial x^2} - \frac{\partial^3 \delta u_x}{\partial y^2 \partial x} - \frac{\partial^3 \delta u_x}{\partial x^3} - \frac{\partial^3 \delta u_y}{\partial y^3} \right], \end{aligned} \quad (\text{A 15})$$

$$\frac{\partial}{\partial t} \frac{\delta n_i}{n_i} + \left(\frac{\partial \delta u_x}{\partial x} + \frac{\partial \delta u_y}{\partial y} \right) + \frac{n'_i}{n_i} \delta u_x = 0, \quad (\text{A 16})$$

$$\begin{aligned} \frac{\partial \delta u_x}{\partial x} + \frac{\partial \delta u_y}{\partial y} + \frac{1}{\Omega_i} \frac{\partial}{\partial t} \left(\frac{\partial \delta u_y}{\partial x} - \frac{\partial \delta u_x}{\partial y} \right) &+ \frac{\nu_i}{\Omega_i} \left[\frac{n'_i}{n_i} \left(\frac{\partial^2 \delta u_x}{\partial x^2} + \frac{\partial^2 \delta u_x}{\partial y^2} \right) \right. \\ &\quad \left. + \frac{\partial^3 \delta u_y}{\partial y \partial x^2} + \frac{\partial^3 \delta u_x}{\partial y^2 \partial x} + \frac{\partial^3 \delta u_x}{\partial x^3} + \frac{\partial^3 \delta u_y}{\partial y^3} \right] = 0. \end{aligned} \quad (\text{A 17})$$

As we expect time-independent growth rates, we can assume the time-dependence of the perturbed quantities to be $e^{i\omega t}$. The perturbed quantities can then be written as:

$$X(\mathbf{r}, t) = \hat{X} e^{ik_y y + ik_x x + i\omega t}. \quad (\text{A 18})$$

Substituting this into (A 15)–(A 17), we obtain

$$\begin{aligned} -\omega \left(k_x \widehat{\delta u}_y - k_y \widehat{\delta u}_x \right) &= ik_y g \frac{\widehat{\delta n}_i}{n_i} + \nu_i \left[2 \frac{n'_i}{n_i} (k_x^2 + k_y^2) \widehat{\delta u}_x \right. \\ &\quad \left. + ik_y k_x^2 \widehat{\delta u}_y + ik_y^2 k_x \widehat{\delta u}_x + ik_x^3 \widehat{\delta u}_x + ik_y^3 \widehat{\delta u}_y \right], \end{aligned} \quad (\text{A 19})$$

$$i\omega \frac{\widehat{\delta n}_i}{n_i} + \left[(ik_x) \widehat{\delta u}_x + (ik_y) \widehat{\delta u}_y \right] + \frac{n'_i}{n_i} \widehat{\delta u}_x = 0, \quad (\text{A 20})$$

$$\begin{aligned} ik_x \widehat{\delta u}_x + ik_y \widehat{\delta u}_y - \frac{\omega}{\Omega_i} \left(k_x \widehat{\delta u}_y - k_y \widehat{\delta u}_x \right) &+ \frac{\nu_i}{\Omega_i} \left[-\frac{n'_i}{n_i} (k_x^2 + k_y^2) \widehat{\delta u}_x \right. \\ &\quad \left. - ik_x^2 k_y \widehat{\delta u}_y - ik_x k_y^2 \widehat{\delta u}_x - ik_x^3 \widehat{\delta u}_x - ik_y^3 \widehat{\delta u}_y \right] = 0. \end{aligned} \quad (\text{A 21})$$

This system of three equations can be solved for the three unknowns $\widehat{\delta u}_x$, $\widehat{\delta u}_y$, and $\widehat{\delta n}_i$, giving us the following dispersion relationship:

$$\begin{aligned} \left(\underbrace{\frac{k_x^2}{k_y^2}}_{\sim 1} - i \underbrace{\frac{\rho_i^2 n'_i k_x}{4 n_i k_y} \frac{k_\perp^2}{k_y^2}}_{\sim \epsilon} + 1 \right) \underbrace{\omega^2}_{\sim \epsilon^2 \Omega_i^2} &+ \left[- \underbrace{(\omega_{gi} + \omega_{*i}) \frac{k_\perp^2}{k_y^2}}_{\sim \epsilon \Omega_i} + i \underbrace{\frac{n'_i}{n_i} \omega_{gi} \frac{k_x}{k_y^2}}_{\sim \epsilon^2 \Omega_i} \right. \\ &\quad \left. + \frac{1}{8} \underbrace{\omega_{*i} \frac{k_\perp^4}{k_y^2} \rho_i^2}_{\sim \epsilon \Omega_i} \right] \underbrace{\omega}_{\sim \epsilon \Omega_i} = - \underbrace{\frac{\omega_{gi} \omega_{*i}}{k_y^2 \rho_i^2 / 2}}_{\sim \epsilon^2 \Omega_i^2}. \end{aligned} \quad (\text{A 22})$$

As before, we retain only up to $\mathcal{O}(\epsilon^2)$. The lowest order i.e. $\mathcal{O}(1)$ gives us

$$\left(\frac{k_x^2}{k_y^2} + 1 \right) \omega^2 = - \frac{\omega_{gi} \omega_{*i}}{k_y^2 \rho_i^2 / 2} \implies \omega^2 = - \frac{\omega_{gi} \omega_{*i}}{k_\perp^2 \rho_i^2 / 2}. \quad (\text{A 23})$$

In other words, equation (A 23) tells us that any finite value of k_x contributes to the stability of the mode. As such, we will set $k_x = 0$ and hence $k_\perp = k_y$ in order to focus on the most unstable modes. Then, retaining only up to $\mathcal{O}(\epsilon^2)$ in (A 22) gives us (3.4).

A.4. Time-dependent finite shear dispersion relation

From (A 11), (A 12), and (A 14) in which $S \neq 0$, we can apply the coordinate transformation (3.7) to obtain:

$$-St' \frac{\partial}{\partial t'} \left(\frac{\partial \delta u_y}{\partial y'} \right) - \frac{\partial}{\partial t'} \frac{\partial \delta u_x}{\partial y'} - S^2 t' \frac{\partial \delta u_x}{\partial y'} = g \frac{\partial}{\partial y'} \left(\frac{\delta n_i}{n_i} \right) + \nu_i \left(S^2 t'^2 + 1 \right) \left[-2 \frac{n'_i}{n_i} \frac{\partial^2 \delta u_x}{\partial y'^2} + St' \frac{\partial^3 \delta u_x}{\partial y'^3} - \frac{\partial^3 \delta u_y}{\partial y'^3} \right] + 2\nu_i S^2 t' \frac{\partial^2}{\partial y'^2} \left(\frac{\delta n_i}{n_i} \right), \quad (\text{A } 24)$$

$$\frac{\partial}{\partial t'} \left(\frac{\delta n_i}{n_i} \right) + \left(-St' \frac{\partial \delta u_x}{\partial y'} + \frac{\partial \delta u_y}{\partial y'} \right) + \frac{n'_i}{n_i} \delta u_x = 0, \quad (\text{A } 25)$$

$$-St' \frac{\partial \delta u_x}{\partial y'} + \frac{\partial \delta u_y}{\partial y'} + \frac{1}{\Omega_i} \left[-St' \frac{\partial}{\partial t'} \left(\frac{\partial \delta u_y}{\partial y'} \right) - \frac{\partial}{\partial t'} \left(\frac{\partial \delta u_x}{\partial y'} \right) - S^2 t' \frac{\partial \delta u_x}{\partial y'} \right] + \frac{\nu_i}{\Omega_i} \left(S^2 t'^2 + 1 \right) \left[\frac{n'_i}{n_i} \frac{\partial^2 \delta u_x}{\partial y'^2} - St' \frac{\partial^3 \delta u_x}{\partial y'^3} + \frac{\partial^3 \delta u_y}{\partial y'^3} \right] - \frac{2\nu_i}{\Omega_i} S^2 t' \frac{\partial^2}{\partial y'^2} \left(\frac{\delta n_i}{n_i} \right) = 0. \quad (\text{A } 26)$$

We assume perturbed quantities of the form $X = \hat{X}(t') e^{ik'_y y'}$ where the quantity X refers to either δu_x , δu_y , or δn_i . After suppressing the primes in the above equations, we obtain:

$$-iSt \frac{\partial \widehat{\delta u_y}}{\partial t} - i \frac{\partial \widehat{\delta u_x}}{\partial t} - iS^2 t \widehat{\delta u_x} = ig \frac{\widehat{\delta n_i}}{n_i} + k_y \nu_i \left(S^2 t^2 + 1 \right) \left(2 \frac{n'_i}{n_i} \widehat{\delta u_x} - iSt k_y \widehat{\delta u_x} + ik_y \widehat{\delta u_y} \right) - 2\nu_i S^2 t k_y \frac{\widehat{\delta n_i}}{n_i}, \quad (\text{A } 27)$$

$$\frac{\partial}{\partial t} \left(\frac{\widehat{\delta n_i}}{n_i} \right) - iSt k_y \widehat{\delta u_x} + ik_y \widehat{\delta u_y} + \frac{n'_i}{n_i} \widehat{\delta u_x} = 0, \quad (\text{A } 28)$$

$$-iSt \widehat{\delta u_x} + i \widehat{\delta u_y} - \frac{i}{\Omega_i} \left(St \frac{\partial \widehat{\delta u_y}}{\partial t} + \frac{\partial \widehat{\delta u_x}}{\partial t} + S^2 t \widehat{\delta u_x} \right) + \frac{k_y \nu_i}{\Omega_i} \left(S^2 t^2 + 1 \right) \left(-\frac{n'_i}{n_i} \widehat{\delta u_x} + iSt k_y \widehat{\delta u_x} - ik_y \widehat{\delta u_y} \right) + \frac{2\nu_i}{\Omega_i} S^2 t k_y \frac{\widehat{\delta n_i}}{n_i} = 0. \quad (\text{A } 29)$$

Equation (A 29) can be multiplied by Ω_i and subtracted from (A 27). The resulting equation can then be combined with (A 28) to give:

$$\widehat{\delta u_x} = \frac{n_i}{n'_i} \frac{\frac{\partial}{\partial t} \left(\frac{\widehat{\delta n_i}}{n_i} \right) - \frac{ig k_y}{\Omega_i} \frac{\widehat{\delta n_i}}{n_i}}{\frac{k_y^2 \nu_i}{\Omega_i} (S^2 t^2 + 1) - 1}, \quad (\text{A } 30)$$

$$\widehat{\delta u_y} = -\frac{g}{\Omega_i} \frac{\widehat{\delta n_i}}{n_i} + \left[i \frac{n'_i}{n_i} \frac{k_y \nu_i}{\Omega_i} (S^2 t^2 + 1) + St \right] \frac{n_i}{n'_i} \frac{\frac{\partial}{\partial t} \left(\frac{\widehat{\delta n_i}}{n_i} \right) - \frac{ig k_y}{\Omega_i} \frac{\widehat{\delta n_i}}{n_i}}{\frac{k_y^2 \nu_i}{\Omega_i} (S^2 t^2 + 1) - 1}. \quad (\text{A } 31)$$

Substituting into (A 27) gives:

$$\begin{aligned}
 0 = & (S^2 t^2 + 1) \underbrace{\left(\frac{i}{2} \frac{\omega_{*i}}{\Omega_i} S t + 1 \right)}_{\sim \epsilon} \underbrace{\frac{\partial^2}{\partial t^2} \left(\frac{\widehat{\delta n}_i}{n_i} \right)}_{\sim \epsilon^3 \Omega_i^2} \\
 & + \left\{ \begin{aligned} & \underbrace{St \frac{1}{\Omega_i} \frac{\omega_{*i} \omega_{gi}}{k_y^2 \rho_i^2 / 2}}_{\sim \epsilon^2 \Omega_i} + \underbrace{i S^3 t^2 \frac{\omega_{*i}}{\Omega_i}}_{\sim \epsilon^2 \Omega_i} + \underbrace{2 S^2 t - i(\omega_{gi} + \omega_{*i})(S^2 t^2 + 1)}_{\sim \epsilon \Omega_i} \\ & + \underbrace{i \frac{k_y^2 \rho_i^2}{8} \omega_{*i} (S^2 t^2 + 1)^2}_{\sim \epsilon \Omega_i} - \underbrace{\frac{k_y^2 \rho_i^2}{2} \frac{1 + \frac{i S t \omega_{*i}}{2 \Omega_i}}{\frac{k_y^2 \rho_i^2}{4} (S^2 t^2 + 1) - 1}}_{\sim \epsilon \Omega_i} S^2 t (S^2 t^2 + 1) \end{aligned} \right\} \underbrace{\frac{\partial}{\partial t} \left(\frac{\widehat{\delta n}_i}{n_i} \right)}_{\sim \epsilon^2 \Omega_i} \\
 & + \left\{ \begin{aligned} & \underbrace{\frac{\omega_{gi} \omega_{*i}}{\Omega_i} S^3 t^2}_{\sim \epsilon^3 \Omega_i^2} - \underbrace{i(2\omega_{gi} + \omega_{*i}) S^2 t}_{\sim \epsilon^2 \Omega_i^2} + \underbrace{2\omega_{*i} \omega_{gi} (S^2 t^2 + 1)}_{\sim \epsilon^2 \Omega_i^2} - \underbrace{\frac{\omega_{gi} \omega_{*i}}{k_y^2 \rho_i^2 / 2}}_{\sim \epsilon^2 \Omega_i^2} \\ & + \underbrace{i \frac{k_y^2 \rho_i^2}{2} \frac{1 + \frac{i \omega_{*i}}{2 \Omega_i} S t}{\frac{k_y^2 \rho_i^2}{4} (S^2 t^2 + 1) - 1}}_{\sim \epsilon^2 \Omega_i^2} \omega_{gi} S^2 t (S^2 t^2 + 1) + \underbrace{i \frac{k_y^2 \rho_i^2}{4} \omega_{*i} S^2 t (S^2 t^2 + 1)}_{\sim \epsilon^2 \Omega_i^2} \end{aligned} \right\} \underbrace{\frac{\widehat{\delta n}_i}{n_i}}_{\sim \epsilon}.
 \end{aligned} \tag{A 32}$$

We retain terms that are only order $\mathcal{O}(\epsilon^3)$ since this is the lowest non-vanishing order of ∂_{tt} on the LHS. This yields:

$$\begin{aligned}
 & (S^2 t^2 + 1) \frac{\partial^2 \widehat{\delta n}_i}{\partial t^2} + \left\{ 2 S^2 t - i(\omega_{gi} + \omega_{*i})(S^2 t^2 + 1) + i \frac{k_y^2 \rho_i^2}{8} \omega_{*i} (S^2 t^2 + 1)^2 \right. \\
 & \left. - \frac{k_y^2 \rho_i^2}{2} \frac{S^2 t (S^2 t^2 + 1)}{\frac{k_y^2 \rho_i^2}{4} (S^2 t^2 + 1) - 1} \right\} \frac{\partial \widehat{\delta n}_i}{\partial t} + \left\{ -i(2\omega_{gi} + \omega_{*i}) S^2 t + i \frac{k_y^2 \rho_i^2}{2} \frac{\omega_{gi} S^2 t (S^2 t^2 + 1)}{\frac{k_y^2 \rho_i^2}{4} (S^2 t^2 + 1) - 1} \right. \\
 & \left. + i \frac{k_y^2 \rho_i^2}{4} \omega_{*i} S^2 t (S^2 t^2 + 1) + 2\omega_{*i} \omega_{gi} (S^2 t^2 + 1) - \frac{\omega_{gi} \omega_{*i}}{k_y^2 \rho_i^2 / 2} \right\} \widehat{\delta n}_i = 0.
 \end{aligned} \tag{A 33}$$

To get (3.10), we only keep terms up to $\mathcal{O}(k_y \rho_i)$.

Appendix B. The role of incompressibility in MHD

We shall demonstrate here how to recover the expressions in Ng & Hassam (2005) by replacing (A 7) with the incompressibility condition $\nabla \cdot \mathbf{U} = 0$. In this case, equations (A 24) and (A 25) still holds, but (A 26) simply reduces to only retaining the first two terms on the LHS:

$$\widehat{\delta u}_y = St \widehat{\delta u}_x. \tag{B 1}$$

Substituting into (A 25) gives us:

$$\widehat{\delta u}_x = -\frac{n_i}{n'_i} \frac{\partial}{\partial t} \left(\frac{\widehat{\delta n}_i}{n_i} \right) \tag{B 2}$$

substituting (B 1) and (B 2) into (A 24) gives us

$$(S^2 t^2 + 1) \frac{\partial^2 \widehat{\delta n}_i}{\partial t^2} + 2S^2 t \frac{\partial \widehat{\delta n}_i}{\partial t} = \frac{\omega_{gi} \omega_{*i}}{k_y^2 \rho_i^2 / 2} \widehat{\delta n}_i + i\omega_{*i} (S^2 t^2 + 1) \frac{\partial \widehat{\delta n}_i}{\partial t} + i\omega_{*i} S^2 t \widehat{\delta n}_i, \quad (\text{B } 3)$$

which is equivalent to equation (16) in Ng & Hassam (2005).

Appendix C. Derivation of the gyrokinetic integral equation

We introduce the integrating factor $e^{i\omega_{gs}t}$ to equation (4.26). This gives us

$$\frac{\partial}{\partial t} \left[e^{i\omega_{gs}t} \widehat{h}_s(t) \right] = \frac{Z_s e F_{0s}}{T_s} e^{i\omega_{gs}t} \left[\frac{\partial}{\partial t} + i(\omega_{gs} + \omega_{*s}) \right] J_0(a_s(t)) \widehat{\delta\varphi}(t). \quad (\text{C } 1)$$

Integrating from 0 to t , we then obtain

$$e^{i\omega_{gs}t} \widehat{h}_s(t) - \widehat{h}_s(0) = \frac{Z_s e F_{0s}}{T_s} \int_0^t dt' e^{i\omega_{gs}t'} \left[\frac{\partial}{\partial t'} + i(\omega_{gs} + \omega_{*s}) \right] J_0(a_s(t')) \widehat{\delta\varphi}(t'), \quad (\text{C } 2)$$

where t' is a dummy variable. The integral on the RHS of (C 2) can be evaluated as

$$\begin{aligned} \int_0^t dt' e^{i\omega_{gs}t'} \left[\frac{\partial}{\partial t'} + i(\omega_{gs} + \omega_{*s}) \right] J_0(a_s(t')) \widehat{\delta\varphi}(t') &= -J_0(a_s(0)) \widehat{\delta\varphi}(0) \\ + e^{i\omega_{gs}t} J_0(a_s(t)) \widehat{\delta\varphi}(t) + i\omega_{*s} \int_0^t dt' e^{i\omega_{gs}t'} &\left[J_0(a_s(t')) \widehat{\delta\varphi}(t') \right]. \end{aligned} \quad (\text{C } 3)$$

Substituting this back into (C 2), we obtain

$$\begin{aligned} \widehat{h}_s(t) &= \widehat{h}_s(0) e^{-i\omega_{gs}t} - \frac{Z_s e F_{0s}}{T_s} e^{-i\omega_{gs}t} J_0(a_s(0)) \widehat{\delta\varphi}(0) + \frac{Z_s e F_{0s}}{T_s} J_0(a_s(t)) \widehat{\delta\varphi}(t) \\ &+ \frac{Z_s e F_{0s}}{T_s} i\omega_{*s} \int_0^t d\Delta t e^{-i\omega_{gs}\Delta t} J_0(a_s(t')) \widehat{\delta\varphi}(t - \Delta t), \end{aligned} \quad (\text{C } 4)$$

where we have introduced another dummy variable $\Delta t = t - t'$.

Plugging (C 4) into (4.27), we obtain

$$\begin{aligned} \sum_s \frac{Z_s^2 e^2 n_s}{T_s} \widehat{\delta\varphi}(t) &= \sum_s Z_s e \int d^3 \mathbf{w} J_0(a_s(t)) e^{-i\omega_{gs}t} \left[\widehat{h}_s(0) - \frac{Z_s e F_{0s}}{T_s} J_0(a_s(0)) \widehat{\delta\varphi}(0) \right] \\ + \sum_s \frac{Z_s^2 e^2 n_s}{T_s} \frac{1}{\pi^{3/2} v_{\text{th},s}^3} &\left\{ \widehat{\delta\varphi}(t) \int d^3 \mathbf{w} e^{-w^2/v_{\text{th},s}^2} \left[J_0(a_s(t)) \right]^2 \right. \\ + i\omega_{*s} \int_0^t d\Delta t e^{-i\omega_{gs}\Delta t} &\widehat{\delta\varphi}(t - \Delta t) \int d^3 \mathbf{w} J_0(a_s(t)) J_0(a_s(t')) e^{-w^2/v_{\text{th},s}^2} \left. \right\}. \end{aligned} \quad (\text{C } 5)$$

The velocity integrals of the second and third terms on the RHS can be evaluated using the identity (4.12), resulting in

$$\begin{aligned} \sum_s \frac{Z_s^2 e^2 n_s}{T_s} \widehat{\delta\varphi}(t) &= \sum_s Z_s e \int d^3 \mathbf{w} J_0(a_s(t)) e^{-i\omega_{gs}t} \left[\widehat{h}_s(0) - \frac{Z_s e F_{0s}}{T_s} J_0(a_s(0)) \widehat{\delta\varphi}(0) \right] \\ + \sum_s \frac{Z_s^2 e^2 n_s}{T_s} &\left[\widehat{\delta\varphi}(t) \Gamma_0(\lambda_s, \lambda_s) + i\omega_{*s} \int_0^t d\Delta t e^{-i\omega_{gs}\Delta t} \Gamma_0(\lambda_s, \lambda'_s) \widehat{\delta\varphi}(t - \Delta t) \right], \end{aligned} \quad (\text{C } 6)$$

where we have used the definitions of Γ_0 and λ_s in (4.29) and (4.30) respectively. Equation (C6) is equivalent to (4.28).

Appendix D. Derivation of the gyrokinetic perturbed ion density equation

D.1. From the integral equation

From the quasineutrality equation (4.27), the perturbed ion density can be defined to be ($Z_i = +1$ for a hydrogen plasma):

$$\widehat{\delta n}_i = -\frac{en_i}{T_i} \widehat{\delta\varphi} + \int d^3\mathbf{w} J_0(a_i(t)) \widehat{h}_i. \quad (\text{D1})$$

As we have done in the derivation of the gyrokinetic integral equation in Appendix C, we need to substitute the equation for \widehat{h}_i in (C4) into (D1). However, the resulting velocity integral is exactly the same as the one calculated in (C5). The result is:

$$\begin{aligned} \widehat{\delta n}_i &= \frac{en_i}{T_i} [\Gamma_0(\lambda_i, \lambda_i) - 1] \widehat{\delta\varphi} + \kappa n_i e^{-i\omega_{gi}t} e^{-\lambda_i(t)/2} \\ &+ \frac{en_i}{T_i} i\omega_{*i} \int_0^t d\Delta t e^{-i\omega_{gi}\Delta t} \Gamma_0(\lambda_i, \lambda'_i) \widehat{\delta\varphi}(t - \Delta t). \end{aligned} \quad (\text{D2})$$

At $t = 0$, we have:

$$\widehat{\delta n}_i(0) = n_i \left\{ \kappa e^{-\lambda_{i0}/2} + \frac{e}{T_i} [\Gamma_0(\lambda_{i0}, \lambda_{i0}) - 1] \widehat{\delta\varphi}(0) \right\}. \quad (\text{D3})$$

Dividing (D2) by (D3), using the definition of $\widehat{\delta\varphi}(0)$ in (4.41), undoing the change of variables $\Delta t = t - t'$, and using the GX normalizations ultimately gives (5.7).

D.2. From GX

Using the GX normalizations, equation (D1) becomes:

$$\widetilde{\delta n}_i = -\widetilde{\delta\varphi} + \int d^3\mathbf{w} J_0(a_i(t)) \widetilde{h}_i. \quad (\text{D4})$$

The first and second quantities can be computed from the `Phi` and `ParticleDensity` diagnostic in GX. An important caveat is that the output of these quantities are in Fourier space and in the lab frame; however, the quantities that we are interested in are in the shearing frame. Fortunately, this is of no issue to us as it is straightforward to connect the shearing frame Fourier amplitudes with that of the lab frame.

To see this, we note that the shearing box transformation (see §3.2.1) ensures that $\mathbf{k} \cdot \mathbf{r} = \mathbf{k}' \cdot \mathbf{r}'$. Using $\delta\varphi$ as an example, the Fourier transform in the shearing frame (4.23) can be more generally written as:

$$\delta\varphi = \sum_{k'_y} \sum_{k'_x} \widehat{\delta\varphi}(t', k'_x, k'_y) e^{ik'_x x'} e^{ik'_y y'} = \sum_{k'_y} \sum_{k'_x} \widehat{\delta\varphi}(t', k'_x, k'_y) e^{ik_x x} e^{ik_y y}. \quad (\text{D5})$$

On the other hand, in the lab frame, we also must have:

$$\delta\varphi = \sum_{k_y} \sum_{k_x} \widehat{\delta\psi}(t', k_x, k_y) e^{ik_x x} e^{ik_y y}. \quad (\text{D6})$$

We are only concerned with $k'_x = 0$ and a single $k'_y = k_y$, so equating (D5) with (D6)

gives:

$$\widehat{\delta\varphi}(t', 0, k'_y) = \sum_{k_x} \widehat{\delta\psi}(t', k'_x, k'_y) e^{ik_x x}, \quad (\text{D7})$$

where we have used the fact that from (3.9), we have $k_x = -St'k'_y$ and $k_y = k'_y$. Since we are interested in the volume average of the quantity (D6), we have:

$$\frac{1}{L_x} \int_0^{L_x} \widehat{\delta\varphi}(t', 0, k'_y) = \sum_{k_x} \left| \widehat{\delta\psi}(t', k'_x, k'_y) \right|^2, \quad (\text{D8})$$

where we have invoked Parseval's theorem. It is the components $\widehat{\delta\psi}(t', k'_x, k'_y)$ that is computed by GX (under the appropriate normalizations).

By this same logic, since (D4) is linear, we can add the complex values of the two diagnostics together on the RHS and then perform the summation as in the RHS of (D8).

Appendix E. Initial conditions for the finite shear MHD equation

The finite shear MHD equation (5.3) requires us to supplement the initial values of $\widetilde{\delta n_i}(\tilde{t})/\widetilde{\delta n_i}(0)$ and its derivative. While the former is clearly 1, the latter needs to be obtained by differentiating (D1):

$$\left. \frac{\partial \widehat{\delta n_i}}{\partial t} \right|_{t=0} = -\frac{en_i}{T_i} \left. \frac{\partial \widehat{\delta\varphi}}{\partial t} \right|_{t=0} + \int d^3\mathbf{w} \left. \frac{\partial}{\partial t} \left[J_0(a_i(t)) \hat{h}_i \right] \right|_{t=0}. \quad (\text{E1})$$

Let us first handle the second term on the RHS of (E1). Using the fact that $J'_0(x) = -J_1(x)$, we can differentiate (C4) to obtain:

$$\begin{aligned} \left. \frac{\partial \hat{h}_i}{\partial t} \right|_{t=0} &= -i\omega_{gi} \hat{h}_i(0) + \frac{eF_{0i}}{T_i} i(\omega_{gi} + \omega_{*i}) J_0(a_i(0)) \widehat{\delta\varphi}(0) \\ &+ \frac{eF_{0i}}{T_i} J_0(a_i(0)) \left. \frac{\partial \widehat{\delta\varphi}(t)}{\partial t} \right|_{t=0} - \frac{eF_{0i}}{T_i} \widehat{\delta\varphi}(0) \left. \frac{\partial a_i(t)}{\partial t} \right|_{t=0} J_1(a_i(0)). \end{aligned} \quad (\text{E2})$$

Using our initial condition (4.37) for the gyrokinetic integral equation and the definitions of λ_i and a_i in (4.30), we obtain:

$$\begin{aligned} \left. \frac{\partial}{\partial t} \left[J_0(a_i(t)) \hat{h}_i \right] \right|_{t=0} &= -i\kappa\omega_{gi} J_0(a_i(0)) F_{0i} + \frac{eF_{0i}}{T_i} [J_0(a_i(0))]^2 \left. \frac{\partial \widehat{\delta\varphi}(t)}{\partial t} \right|_{t=0} \\ &+ i\omega_{*i} \frac{e\widehat{\delta\varphi}(0)}{T_i} [J_0(a_i(0))]^2 F_{0i}. \end{aligned} \quad (\text{E3})$$

The velocity integration then gives:

$$\begin{aligned} \int d^3\mathbf{w} \left. \frac{\partial}{\partial t} \left[J_0(a_i(t)) \hat{h}_i \right] \right|_{t=0} &= \frac{en_i}{T_i} \left[\left. \frac{\partial \widehat{\delta\varphi}(t)}{\partial t} \right|_{t=0} + i\omega_{*i} \widehat{\delta\varphi}(0) \right] \Gamma_0(\lambda_{i0}, \lambda_{i0}) \\ &- i\kappa\omega_{gi} n_i e^{-\lambda_{i0}/2}. \end{aligned} \quad (\text{E4})$$

The first term on the RHS of (E1) can be calculated directly from the integral equation (4.42) where it suffices to take the small mass ratio approximation $m_e/m_i \ll 1$ as it is an MHD calculation:

$$\widehat{\delta\varphi}(t) \approx \frac{\kappa T_i}{e} \frac{e^{-\lambda_i/2} e^{-i\omega_{gi}t} - 1}{1 - \Gamma_0(\lambda_i, \lambda_i)} + i\omega_{*i} \int_0^t dt' \frac{e^{-i\omega_{gi}(t-t')} \Gamma_0(\lambda_i, \lambda'_i) - 1}{1 - \Gamma_0(\lambda_i, \lambda_i)} \widehat{\delta\varphi}(t'). \quad (\text{E5})$$

By noting that $I'_0(x) = I_1(x)$, we have:

$$\frac{\partial}{\partial t} \Gamma_0(\lambda_i, \lambda'_i) = \frac{1}{2} \Gamma_0(\lambda_i, \lambda'_i) \left[\frac{1}{\sqrt{\lambda_i \lambda'_i}} \frac{I_1(\sqrt{\lambda_i \lambda'_i})}{I_0(\sqrt{\lambda_i \lambda'_i})} \lambda'_i - 1 \right] \frac{\partial \lambda_i}{\partial t}, \quad (\text{E6})$$

$$\frac{\partial}{\partial t} \Gamma_0(\lambda_i, \lambda_i) = \frac{\partial \lambda_i}{\partial t} \left[\frac{I_1(\lambda_i)}{I_0(\lambda_i)} - 1 \right] \Gamma_0(\lambda_i, \lambda_i). \quad (\text{E7})$$

This allows us to differentiate (E5) and obtain:

$$\begin{aligned} \frac{\partial}{\partial t} \widehat{\delta\varphi}(t) &= \frac{\kappa T_i/e}{1 - \Gamma_0(\lambda_i, \lambda_i)} \left[- \left(\frac{1}{2} \frac{\partial \lambda_i}{\partial t} + i\omega_{gi} \right) e^{-\lambda_i/2} e^{-i\omega_{gi}t} + \frac{e^{-\lambda_i/2} e^{-i\omega_{gi}t} - 1}{1 - \Gamma_0(\lambda_i, \lambda_i)} \frac{\partial \Gamma_0(\lambda_i, \lambda_i)}{\partial t} \right] \\ &+ i\omega_{*i} \left\{ \int_0^t dt' \left[e^{-i\omega_{gi}(t-t')} \Gamma_0(\lambda_i, \lambda'_i) - 1 \right] \widehat{\delta\varphi}(t') \right\} \frac{\partial}{\partial t} \frac{1}{1 - \Gamma_0(\lambda_i, \lambda_i)} \\ &- i\omega_{*i} \widehat{\delta\varphi}(t) + \frac{i\omega_{*i}}{1 - \Gamma_0(\lambda_i, \lambda_i)} \int_0^t dt' \frac{\partial}{\partial t} \left\{ \left[e^{-i\omega_{gi}(t-t')} \Gamma_0(\lambda_i, \lambda'_i) - 1 \right] \widehat{\delta\varphi}(t') \right\}, \end{aligned} \quad (\text{E8})$$

and hence:

$$\left. \frac{\partial}{\partial t} \widehat{\delta\varphi}(t) \right|_{t=0} = - \frac{\kappa T_i}{e} \frac{i\omega_{gi}}{1 - \Gamma_0(\lambda_{i0}, \lambda_{i0})} e^{-\frac{\lambda_{i0}}{2}} - i\omega_{*i} \widehat{\delta\varphi}(0). \quad (\text{E9})$$

Substituting the results (E4) and (E9) into (E1), we obtain:

$$\left. \frac{\partial}{\partial t} \frac{\widehat{\delta n}_i}{n_i} \right|_{t=0} = i\kappa\omega_{*i} \frac{e^{-\frac{\lambda_{i0}}{2}} - 1}{1 - \Gamma_0(\lambda_{i0}, \lambda_{i0})}, \quad (\text{E10})$$

where we have used and taken the small mass ratio $m_e/m_i \ll 1$ of $\widehat{\delta\varphi}(0)$ given in (4.41). In addition, this also allows us to obtain $\widehat{\delta n}_i(0) \approx \kappa n_i$ from (D3), for which we can then rewrite (E10) as:

$$\left. \frac{\partial}{\partial t} \frac{\widehat{\delta n}_i}{\widehat{\delta n}_i(0)} \right|_{t=0} = i\omega_{*i} \frac{e^{-\frac{\lambda_{i0}}{2}} - 1}{1 - \Gamma_0(\lambda_{i0}, \lambda_{i0})}. \quad (\text{E11})$$

Taking the long-wavelength limit $\lambda_{i0} \ll 1$ and using the GX normalizations, we finally arrive at:

$$\left. \frac{\partial}{\partial t} \frac{\widetilde{\delta n}_i}{\widetilde{\delta n}_i(0)} \right|_{t=0} \approx -i \frac{\widetilde{\omega}_{*i}}{2}. \quad (\text{E12})$$

It is this expression we shall use to compute our initial derivative for the finite shear MHD equation.

Appendix F. Low order GK expansions

F.1. Electrostatic potential equation

Taking the $m_e/m_i = \widetilde{m}_e \ll 1$ limit of the integral equation for $\widetilde{\delta\varphi}$ (5.4) gives:

$$\begin{aligned} \frac{\widetilde{\delta\varphi}(\widetilde{t})}{\widetilde{\delta\varphi}(0)} &= \frac{e^{-\lambda_i/2} e^{-i\widetilde{\omega}_{gi}\widetilde{t}} - 1}{e^{-\lambda_{i0}/2} - 1} \frac{1 - \Gamma_0(\lambda_{i0}, \lambda_{i0})}{1 - \Gamma_0(\lambda_i, \lambda_i)} \\ &+ i\widetilde{\omega}_{*i} \int_0^{\widetilde{t}} d\widetilde{t}' \frac{e^{-i\widetilde{\omega}_{gi}(\widetilde{t}-\widetilde{t}')} \Gamma_0(\lambda_i, \lambda'_i) - 1}{1 - \Gamma_0(\lambda_i, \lambda_i)} \frac{\widetilde{\delta\varphi}(\widetilde{t}')}{\widetilde{\delta\varphi}(0)}. \end{aligned} \quad (\text{F1})$$

Next, by assuming $\tilde{k}_y \ll 1$ and hence $\lambda_i, \lambda'_i \sim \tilde{k}_y^2 \ll 1$, we have:

$$\Gamma_0(\lambda_i, \lambda_i) \approx 1 - \lambda_i + \frac{3}{4}\lambda_i^2, \quad (\text{F } 2)$$

$$\Gamma_0(\lambda_i, \lambda'_i) \approx 1 - \frac{\lambda_i + \lambda'_i}{2} + \frac{\lambda_i^2 + \lambda_i'^2}{8} + \frac{\lambda_i \lambda'_i}{2}. \quad (\text{F } 3)$$

Noting that $\tilde{\omega}_{gi} \sim \tilde{\omega}_{*i} \sim \tilde{k}_y$, equation (F 1) to $\mathcal{O}(\tilde{k}_y)$ is given by:

$$\begin{aligned} \frac{\tilde{\delta\varphi}(\tilde{t})}{\tilde{\delta\varphi}(0)} = & -\frac{2}{\lambda_i} \left(-i\tilde{\omega}_{gi}\tilde{t} - \frac{\tilde{\omega}_{gi}^2\tilde{t}^2}{2} + \frac{i\tilde{\omega}_{gi}^3\tilde{t}^3}{6} \right) - \frac{5}{2} (1 - i\tilde{\omega}_{gi}\tilde{t}) + \frac{3}{2} + \frac{1}{2} \frac{\lambda_{i0}}{\lambda_i} i\tilde{\omega}_{gi}\tilde{t} \\ & + i\tilde{\omega}_{*i} \int_0^{\tilde{t}} d\tilde{t}' \frac{\tilde{\delta\varphi}(\tilde{t}')}{\tilde{\delta\varphi}(0)} \left[-\frac{1}{2} - \frac{\lambda'_i}{2\lambda_i} - \frac{i\tilde{\omega}_{gi}}{\lambda_i} (\tilde{t} - \tilde{t}') - \frac{1}{2\lambda_i} \tilde{\omega}_{gi}^2 (\tilde{t} - \tilde{t}')^2 \right]. \end{aligned} \quad (\text{F } 4)$$

F.2. Perturbed density equation

We now need to repeat the procedure for the perturbed density equation (5.7). The result is:

$$\frac{\tilde{\delta n}_i}{\tilde{\delta n}_i(0)} \approx 1 - i\tilde{\omega}_{gi}\tilde{t} - \frac{i\tilde{\omega}_{*i}}{2} \int_0^{\tilde{t}} d\tilde{t}' \frac{\tilde{\delta\varphi}(\tilde{t}')}{\tilde{\delta\varphi}(0)}. \quad (\text{F } 5)$$

The combination of (F 4) and (F 5) allows us to obtain the grey line in Figure 4.

REFERENCES

- ABEL, I. G., BARNES, M., COWLEY, S. C., DORLAND, W. & SCHEKOCIHIN, A. A. 2008 Linearized model Fokker–Planck collision operators for gyrokinetic simulations. I. Theory. *Phys. Plasmas* **15**, 122509.
- ABEL, I. G., PLUNCK, G. G., WANG, E., BARNES, M., COWLEY, S. C., DORLAND, W. & SCHEKOCIHIN, A. A. 2013 Multiscale gyrokinetics for rotating tokamak plasmas: fluctuations, transport and energy flows. *Rep. Prog. Phys.* **76**, 116201.
- ABRAMOWITZ, M. & STEGUN, I. A. 1970 *Handbook of Mathematical Functions with Formulas, Graphs, and Mathematical Tables*. U.S. Dept. of Commerce, National Bureau of Standards.
- ANTONSEN, T. M. & LANE, B. 1980 Kinetic equations for low frequency instabilities in inhomogeneous plasmas. *Phys. Fluids* **23**, 1205–1214.
- ARIEL, P. D. & BHATIA, P. J. 1969 Effect of finite Larmor radius on Rayleigh–Taylor instability of a plasma. *Can. J. Phys.* **47**, 2435–2437.
- ARTUN, M. & TANG, W. M. 1992 Gyrokinetic analysis of ion temperature gradient modes in the presence of sheared flows. *Phys. Fluids B* **4**, 1102–1114.
- BARNES, M., PARRA, F. I., HIGHCOCK, E. G., SCHEKOCIHIN, A. A., COWLEY, S. C. & ROACH, C. M. 2011 Turbulent Transport in Tokamak Plasmas with Rotational Shear. *Phys. Rev. Lett.* **106**, 175004.
- BIGLARI, H., DIAMOND, P. H. & TERRY, P. W. 1990 Influence of sheared poloidal rotation on edge turbulence. *Phys. Fluids B* **2**, 1–4.
- BOWERS, E. & HAINES, M. G. 1968 Fluid Equations for a Collisionless Plasma including Finite Ion Larmor Radius and Finite β Effects. *Phys. Fluids* **11**, 2695–2708.
- BRAGINSKII, S. I. 1965 TRANSPORT PROCESSES IN A PLASMA. In *Reviews of Plasma Physics* (ed. Acad. M. A. Leontovich), pp. 205–309. Consultants Bureau, New York.
- CATTO, P. J., TANG, W. M. & BALDWIN, D. 1981 Generalized Gyrokinetics. *Plasma Phys.* **23**, 639–650.
- ELLIS, R. F., HASSAM, A. B., MESSER, S. & OSBORN, B. R. 2001 An experiment to test centrifugal confinement for fusion. *Phys. Plasmas* **8**, 2057–2065.
- FERRARO, N. M. 2006 Finite element implementation of Braginskii’s gyroviscous stress with application to the gravitational instability. *Phys. Plasmas* **13**, 092101.

- FERRARO, N. M. 2007 FINITE LARMOR RADIUS EFFECTS ON THE MAGNETOROTATIONAL INSTABILITY. *Astrophys. J.* **662**, 512–516.
- FOX, M. J., VAN WYK, F., FIELD, A. R., GHIM, Y., PARRA, F. I., SCHEKOCIHIN, A. A. & THE MAST TEAM 2017 Symmetry breaking in MAST plasma turbulence due to toroidal flow shear. *Plasma Phys. Control. Fusion* **59**, 034002.
- FRIEMEN, E. A. & CHEN, L. 1982 Nonlinear gyrokinetic equations for low-frequency electromagnetic waves in general plasma equilibria. *Phys. Fluids* **25**, 502–508.
- GOLDSTON, R. J. & RUTHERFORD, P. H. 1995 *Introduction to Plasma Physics*. IOP Publishing Ltd.
- HASSAM, A. B. 1992 Nonlinear stabilization of the Rayleigh-Taylor instability by external velocity shear. *Phys. Fluids B* **4**, 485–487.
- HASSAM, A. B. 1997 Steady State Centrifugally Confined Plasmas for Fusion. *Comments in Plasma Phys. Control. Fusion* **18**, 263–279.
- HIGHCOCK, E. G., BARNES, M., PARRA, F. I., SCHEKOCIHIN, A. A., ROACH, C. M. & COWLEY, S. C. 2011 Transport bifurcation induced by sheared toroidal flow in tokamak plasmas. *Phys. Plasmas* **18**, 102304.
- HIGHCOCK, E. G., BARNES, M., SCHEKOCIHIN, A. A., PARRA, F. I., ROACH, C. M. & COWLEY, S. C. 2010 Transport Bifurcation in a Rotating Tokamak Plasma. *Phys. Rev. Lett.* **105**, 215003.
- HOBBS, C. G., HOUSE, M. G., LEBOEUF, J. N., DAWSON, J. M., DECYK, V. K., KISSICK, M. W. & SYDORA, R. D. 2001 Effect of sheared toroidal rotation on ion temperature gradient turbulence and resistive kink stability in a large aspect ratio tokamak. *Phys. Plasmas* **8**, 4849–4855.
- HUANG, Y. M. & HASSAM, A. B. 2001 Velocity Shear Stabilization of Centrifugally Confined Plasma. *Phys. Rev. Lett.* **87**, 235002.
- HUBA, J. D. 1996 Finite Larmor radius magnetohydrodynamics of the Rayleigh-Taylor instability. *Phys. Plasmas* **3**, 2523–2532.
- IVANOV, P. G., ADKINS, T., KENNEDY, D., GIACOMIN, M., BARNES, M. & SCHEKOCIHIN, A. A. 2025 Suppression of temperature-gradient-driven turbulence by sheared flows in fusion plasmas. *J. Plasma Phys.* **91**, e58.
- KRUSKAL, M. & SCHWARZSCHILD, M. 1954 Some instabilities of a completely ionized plasma. *Proc. Roy. Soc. A* **223**, 348–360.
- LANDREMAN, M., PLUNK, G. G. & DORLAND, W. 2015 Generalized universal instability: transient linear amplification and subcritical turbulence. *J. Plasma Phys.* **81**, 90581051.
- LEHNERT, B. 1971 Rotating Plasmas. *Nucl. Fus.* **11**, 485–533.
- LEVITT, B. J. 2004 Global Mode Analysis of Centrifugal and Curvature Driven Interchange Instabilities. PhD thesis, Columbia University.
- LINZ, P. 1985 *Analytical and Numerical Methods for Volterra Equations*. SIAM Studies in Applied Mathematics.
- MANDELL, N. R., DORLAND, W. D., ABEL, I., GAUR, R., KIM, P., MARTIN, M. & QIAN, T. 2024 GX: a GPU-native gyrokinetic turbulence code for tokamak and stellarator design. *J. Plasma Phys.* **90**, 905900402.
- MANDELL, N. R., DORLAND, W. D. & LANDREMAN, M. 2018 Laguerre–Hermite pseudo-spectral velocity formulation of gyrokinetics. *J. Plasma Phys.* **84**, 905840108.
- NEWTON, S. L., COWLEY, S. C. & LOUREIRO, N. F. 2010 Understanding the effect of sheared flow on microinstabilities. *Plasma Phys. Control. Fusion* **52**, 125001.
- NG, S. & HASSAM, A. B. 2005 Finite Larmor radius assisted velocity shear stabilization of the interchange instability in magnetized plasmas. *Phys. Plasmas* **12**, 064504.
- PARRA, F. I. 2019 Collisional plasma physics. <http://www-thphys.physics.ox.ac.uk/people/FelixParra/> lecture Notes for an Oxford MMathPhys course.
- POLI, F. M., RICCI, P., FASOLI, A. & PODESTÀ, M. 2008 Transition from drift to interchange instabilities in an open magnetic field line configuration. *Phys. Plasmas* **15**, 032104.
- ROBERTS, K. V. & TAYLOR, J. B. 1962 MAGNETOHYDRODYNAMIC EQUATIONS FOR FINITE LARMOR RADIUS. *Phys. Rev. Lett.* **8**, 197–198.
- ROSENBLUTH, M. N., KRALL, N. A. & ROSTOKER, N. 1962 FINITE LARMOR RADIUS STABILIZATION OF “WEAKLY” UNSTABLE CONFINED PLASMAS. *Nucl. Fusion Suppl.* p. 4808729.

- ROSENBLUTH, M. N. & LONGMIRE, C. L. 1957 Stability of Plasmas Confined by Magnetic Fields. *Ann. Phys. (N.Y.)* **1**, 120–140.
- ROSENBLUTH, M. N. & SIMON, A. 1965 Finite Larmor Radius Equations with Nonuniform Electric Fields and Velocities. *Phys. Fluids* **8**, 1300–1322.
- SCHEKOCHIHIN, A. A., COWLEY, S. C., DORLAND, W., HAMMETT, G. W., HOWES, G. G., QUATAERT, E. & TATSUNO, T. 2009 ASTROPHYSICAL GYROKINETICS: KINETIC AND FLUID TURBULENT CASCADES IN MAGNETIZED WEAKLY COLLISIONAL PLASMAS. *Astrophys. J. Suppl.* **182**, 310–377.
- SCHEKOCHIHIN, A. A., HIGHCOCK, E. G. & COWLEY, S. C. 2012 Subcritical fluctuations and suppression of turbulence in differentially rotating gyrokinetic plasmas. *Plasma Phys. Control. Fusion* **54**, 055011.
- SCHNACK, D. D., BARNES, D. C., BRENNAN, D. P., HEGNA, C. C., HELD, E., KIM, C. C., KRUGER, S. E., PANKIN, A. Y. & SOVINEC, C. R. 2006 Computational modeling of fully ionized magnetized plasmas using the fluid approximation. *Phys. Plasmas* **13**, 058103.
- TATSUNO, T., WAKATANI, M. & ICHIGUCHI, K. 1999 Ideal interchange instabilities in stellarators with a magnetic hill. *Nucl. Fusion* **39**, 1391.
- TEODORESCU, C., CLARY, R., ELLIS, R. F., HASSAM, A. B. & LUNSFORD, R. 2008 Experimental study on the velocity limits of magnetized rotating plasmas. *Phys. Plasmas* **15**, 042504.
- THOMPSON, W. B. 1961 The dynamics of high temperature plasmas. *Rep. Prog. Phys.* **24**, 363–424.
- WAKATANI, M., NAKAMURA, Y. & ICHIGUCHI, K. 1992 MHD instabilities in heliotron/torsatron. *Fusion Eng. Des.* **15**, 395–413.
- WALTZ, R. E., DEWAR, R. L. & GARBET, X. 1998 Theory and simulation of rotational shear stabilization of turbulence. *Phys. Plasmas* **5**, 1784–1792.
- XU, R. & KUNZ, M. W. 2016 Linear Vlasov theory of a magnetised, thermally stratified atmosphere. *J. Plasma Phys.* **82**, 905820507.
- ZAGÓRSKI, R., GERHAUSER, H. & CLAASSEN, H. A. 1999 Numerical analysis of plasma instabilities in the TEXTOR tokamak edge plasma. *J. Nucl. Mater* **266–269**, 1261–1266.